PHYSICAL REVIEW D VOLUME 39, NUMBER 3 1 FEBRUARY 1989

Semileptonic B and D decays in the quark model

Nathan Isgur and Daryl Scora
Department of Physics, University of Toronto, Toronto, Canada M5S 1A7

Benjamin Grinstein* and Mark B. Wise
California Institute of Technology, Pasadena, California 91125
(Received 30 June 1988)

We predict the matrix elements and resulting electron spectra for semileptonic meson decays using the quark potential model. Particular attention is paid to the high-energy electron end-point region in B decay since it is crucial to a determination of the $b\to u$ weak mixing angle. It is argued that in this region the usual inclusive ("quark decay") calculations are unjustified and must be replaced by explicit sums over decays of the original meson into low-mass exclusive hadronic final states.

I. PREFACE

Soon after the experimental discovery[1] of some difficulties with the "quark decay" model[2] for the high-energy end point of the electron spectrum in $\bar{B}\to Xe\bar{\nu}_e$, three of us published[3] a critique of the use of the model in that region along with a recalculation of the end-point spectrum based on an explicit summation (via the quark potential model) of the spectra due to the low-massed hadronic resonances which contribute there.

The details of this calculation and of our misgivings concerning the alternatives to it, although available,[4] were not published. In the meantime, several factors led us to decide to publish an expanded and revised version of these details. One is that we have completed new calculations which allow us to confirm some speculations made in our earlier work.[3,4] We now also have a better understanding of the precise relationship of the "quark decay" calculations to ours, and as a result we are in a position to expand considerably upon the reasons for preferring (at least in principle) our approach. Finally, a recent investigation[5] within the framework of our approach has uncovered a potentially serious uncertainty in our calculations. We would also like to address this issue, correcting in the process a mistake in our previous work.

II. INTRODUCTION

In the standard model, based on the gauge group $SU(3)\times SU(2)\times U(1)$, the quarks couple to the W bosons through the weak current

$$J^\mu=\frac{g_2}{2\sqrt{2}}\bar{u}_i\gamma^\mu(1-\gamma_5)V_{ij}d_j\equiv\frac{g_2}{2\sqrt{2}}V_{ij}j^\mu_{ij}\ . \tag{1}$$

In Eq. (1), $i,j\in\{1,\ldots,n\}$ are generation indices and V_{ij} is an $n\times n$ unitary matrix that arises from diagonalization of the quark mass matrices. At present there is experimental evidence for three generations of quarks and leptons. In this case it is possible,[6] by redefining the phases of quark fields, to write V in terms of three angles θ_1, θ_2, θ_3 and a phase δ:

$$V=\begin{bmatrix} c_1 & -s_1c_3 & -s_1s_3 \\ s_1c_2 & c_1c_2c_3-s_2s_3e^{i\delta} & c_1c_2s_3+s_2c_3e^{i\delta} \\ s_1s_2 & c_1s_2c_3+c_2s_3e^{i\delta} & c_1s_2s_3-c_2c_3e^{i\delta} \end{bmatrix}. \tag{2}$$

Here, $c_i\equiv\cos\theta_i$, $s_i\equiv\sin\theta_i$, and the angles θ_i are chosen to lie in the first quadrant.

In the standard model the elements of the matrix V_{ij} are fundamental parameters and their values must be determined experimentally. Information on θ_1 comes from nuclear β decay and semileptonic hyperon decays, whilst information on the angles θ_2 and θ_3 can be obtained from semileptonic B-meson decays. The differential rate for semileptonic $\bar{B}$-meson decay ($\bar{B}^0=-b\bar{d}$, $B^-=b\bar{u}$) has the form ($V_{13}\equiv V_{ub}$ and $V_{23}\equiv V_{cb}$)

$$d\Gamma(\bar{B}\to Xe\bar{\nu})=|V_{cb}|^2d\hat{\Gamma}(\bar{B}\to X_ce\bar{\nu}) +|V_{ub}|^2d\hat{\Gamma}(\bar{B}\to X_ue\bar{\nu})\ , \tag{3}$$

where $d\hat{\Gamma}(\bar{B}\to X_qe\bar{\nu})$ denotes the contribution to $d\Gamma(\bar{B}\to Xe\bar{\nu})$ from the part of the weak current (excluding the weak-mixing angles) where a bottom quark b couples to a quark $q=c$ or u. If the functions $d\hat{\Gamma}(\bar{B}\to X_ce\bar{\nu})$ and $d\hat{\Gamma}(\bar{B}\to X_ue\bar{\nu})$ can be predicted theoretically, then the experimental electron spectrum can be used with Eq. (3) to determine the ratio $|V_{ub}|^2/|V_{cb}|^2$, whilst the absolute semileptonic decay rate can be used to determine the magnitudes of these weak mixing angles. In particular, the contribution to $\Gamma(\bar{B}\to Xe\bar{\nu})$ coming from the $b\to u$ coupling can, in principle, be isolated experimentally by examining the electron spectrum $d\Gamma/dE_e$ in the end-point region near the maximum allowed electron energy, since only $b\to u$ can contribute for $E_e>(m_B^2-m_D^2)/(2m_B)$.

In the free-quark decay model where the b quark decays freely from rest,

$$\hat{\Gamma}(\bar{B}\to X_q e\bar{\nu})=\frac{G_F^2 m_b^5}{192\pi^3} f(m_q/m_b)\ , \tag{4}$$

where $f(x)=1-8x^2+8x^6-x^8-24x^4\ln x$. This free-quark decay model (with and without perturbative QCD corrections[2]) has become the traditional tool for discussing semileptonic decays of heavy quarks. It is known to give a satisfactory understanding of many of the features of such decays, including a semiquantitative description of their absolute rates and good predictions for semileptonic branching ratios. Perhaps for this reason it was hoped that this simple model could also be applied to the prediction of the shape and normalization of the $\bar{B}\to Xe\bar{\nu}_e$ end-point spectrum. This paper and our earlier ones[3,4] are motivated by our belief that the use of the free-quark decay model cannot be justified in precisely this region.

Whilst our reasons for rejecting the free-quark decay model[2] are not very subtle, our point of view is sufficiently iconoclastic for us to feel that it is essential to discuss them fully. The focus of our concerns is the fact that the end-point region is, from kinematics alone, populated via the production of low-mass hadronic systems. In such circumstances the free-quark decay model will suffer from both kinematical and closely related dynamical problems.

Let us begin with an illustration. Imagine a world in which pair creation by the strong interaction is suppressed. (This imaginary world corresponds to QCD in the large-N_c limit. Alternatively, we can view it as an approximation in which QCD is first solved in fixed sectors of Fock space with mixing between sectors treated as a perturbation.) Then the decay $\bar{B}\to Xe\bar{\nu}_e$ will be saturated by hadronic systems X which are $q\bar{q}$ resonances. If, for simplicity, we ignore the motion of the quarks in the decaying $\bar{B}$ meson, then in the free-quark decay model the recoil hadronic mass $m_X^2=(p_{\bar{B}}-p_e-p_{\bar{\nu}})^2$ will be treated as continuously distributed from a minimum value $(m_q+m_d)^2$ up to a maximum value $(m_q+m_d)^2+[(m_d/m_b)(m_b-m_q)^2]$. On the other hand, in our illustrative world the quark q would be captured into one of the discrete eigenstates in which $q\bar{q}$ form a confined meson spectroscopy. In these circumstances, the free-quark differential decay rates will approximately hold (in an energy average sense) in only those regions of phase space where the density of confined states has approached that of the continuum. This corresponds to the usual parton model condition that $p_q\gg 1$ GeV/c. However, at low m_X the "true" hadronic recoil spectrum will be controlled by a sparse set of discrete states which will at best only remotely resemble the free spectrum: $d\Gamma/dm_X^2$ in this region will consist of a set of well-separated spikes. We therefore see that in this limit (large N_c or treating pair creation as a perturbation), on purely kinematical grounds the free-quark decay model cannot possibly reproduce the differential spectrum $d\Gamma/dm_X^2$ at low m_X^2. While $d\Gamma/dm_X^2$ is not a very useful quantity experimentally, this failure reflects directly on the high-energy end-point region of the electron spectrum $d\Gamma/dE_e$. The electron energy spectrum can be viewed as a superposition of m_X-dependent projections of the three-body Dalitz plots for $\bar{B}\to Xe\bar{\nu}_e$ for fixed m_X, each with their corresponding end points $E_e^{\max}=(m_B^2-m_X^2)/2m_B$, so that, as already stated, low m_X determines the high-E_e spectrum. Of course, one might hope that the parton model "averaging" of the confined spectrum will extrapolate right down to the minimum allowed hadronic mass m_X. This "averaging" would necessarily be rather crude, since as each new discrete m_X begins to contribute to the electron spectrum (as the energy drops below its end point), it has associated with it a threshold—with its prescribed threshold behavior—of which the free-quark decay model is completely ignorant. Even allowing for this failure, we can see no justification for such an optimistic view of the range of validity of the free-quark decay model. Its kinematic failures are, after all, a superficial reflection of the deeper dynamical problem of failing to take into account the strong, nonperturbative interactions which create the confined spectrum. In other words, in the low-m_X part of the spectrum there is no justification for the parton model mnemonic that "the short-distance physics determines the inclusive cross section; everything else happens with unit probability."

Before leaving the world of our illustrative example, let us pause to consider a few particulars of semileptonic decays. In $b\to c$ decays, the free-quark m_X spectrum in the above model (with typical quark masses given in the body of the paper below) ranges continuously from 2.15 GeV/c^2 to 2.31 GeV/c^2, whilst the experimental spectrum seems to be dominated by D and D^* production at the two (nearly) discrete masses of 1.87 GeV/c^2 and 2.02 GeV/c^2. Although the continuous spectrum can be arranged—by sensible but nevertheless *ad hoc* manipulations of the free-quark decay model[2]—to give the correct E_e end point and thereby to correspond to an m_X spectrum more closely related to the experimental one, the observed dominance of the D and D^* must *in itself* be viewed as antithetical to the parton-model approximations. We can certainly see no reason to expect the parton model to serve in these circumstances as anything more than a rough guide in the "duality" sense mentioned above. [Note that absolute semileptonic rate predictions of the free-quark decay model are in any event not very significant since, for example, as m_b is varied by ± 300 MeV/c^2 around 5 GeV/c^2, the free-quark rate, Eq. (4), for $\bar{B}\to X_c e\bar{\nu}_e$ varies by about a factor of 2.] In $b\to u$ decay, the corresponding range in m_X is 0.66 GeV/c^2 to 1.38 GeV/c^2, so that— given especially that the motion of the initial quarks will broaden this range—it is justified to expect that the parton-model approximations will be valid at high m_X, where the light-quark spectrum has become reasonably dense. Since hadronic form factors lead to E_e spectra which peak just below the maximum for a given m_X (see below), this corresponds to an applicability of the free b-quark decay model at low E_e in the $b\to u$ spectrum. There is, however, still no justification, even here, for the use of this model at the highest E_e corresponding to the lowest m_X. For example, in the resonance approximation, only the projections of the π and ρ Dalitz plots will contribute to the electron spectrum for $E_e\gtrsim 2.49$ GeV (where the $L=1$ resonances

clustered around 1.25 GeV can no longer contribute), with the ρ contribution cutting off at 2.58 GeV whilst the π contributes all the way to the physical end point at 2.63 GeV. In the free-quark decay model this end-point region receives (pointlike) contributions from the entire section of the Dalitz plot in which the recoiling light quark u and the $\bar{\nu}_e$ are approximately collinear, so that the total rate actually peaks very near the maximum allowed E_e: with the typical constituent-quark masses we use below, the free-quark rate peaks only 0.15 GeV below the end point. However, it seems likely that in nature (as in the model we present below), contributions in this region are suppressed because the π and ρ are soft hadronic objects. Since their momentum-space wave functions have mean momenta of the order of 300 MeV/c, form factors will give very little amplitude for their formation when the collinear u and $\bar{\nu}_e$ contain a high-momentum u quark ($|\mathbf{p}_u|$ from free-quark decay ranges from zero to about 2.5 GeV/c in the b rest frame or from zero to about 0.6 GeV/c in the m_X rest frame). The pointlike amplitude for producing these high–three-momentum u quarks in a pseudoscalar or vector combination with the "spectator" $\bar{d}$ quark is not, of course, lost: it feeds the amplitudes for producing excited states of the π and ρ. However, since elementary kinematics forbids the main effects of these pointlike amplitudes to appear at the highest E_e, the peaking of the electron spectrum will be shifted to lower values.

Despite this failure to describe the spectrum at high E_e, we should emphasize that in this picture the free-quark decay model (and the ancillary QCD jet model) would hold as an approximation which would become increasingly accurate as the mass of the decaying b quark increased. In particular, we note that the range of hadronic masses populated by the decay with a light-quark spectator leads to *all* the thresholds falling within a region δE just below the maximum energy, which becomes an increasingly small fraction of the total E_e range: as $m_b \to \infty$,

$$\frac{\delta E}{E_e^{\max}} \simeq \frac{m_d}{m_b}$$

(we once again neglect quark motion in the hadrons). This happens even though the highest-mass m_X being produced is becoming large: as $m_b \to \infty$,

$$m_X^{\max} \simeq (m_d m_b)^{1/2} .$$

The crucial point is that the model does not produce states with m_X ranging up to $m_B \simeq m_b + m_d$ as allowed by pure kinematics, but rather (as $m_b \to \infty$) only over an infinitesimal fraction of this range. Thus we see that there is, for example, no paradox in producing high-momentum jets through "soft" $q\bar{q}$ bound states: the jets of highest momentum ($\sim \frac{1}{2} m_B$) correspond to large recoils sustained by states which have a density approaching that of the continuum and masses around $(m_d m_b)^{1/2} \ll m_B$, in which the quarks each have mean center-of-mass momenta of $\frac{1}{2}(m_d m_b)^{1/2}$ corresponding, in the original B rest frame, to a recoil quark momentum of $\frac{1}{2} m_B$.

In our discussion of the free b-quark decay model, we have so far neglected perturbative QCD corrections. Gluon radiation will, with a probability of order $\alpha_s(m_b)/\pi$, populate hadronic final states with all masses up to the kinematic limit and thereby produce effects which are missing from our earlier picture. However, if the free b-quark decay picture is to be at all useful, the b-quark mass must be large enough for these effects to be only a small perturbation. Also, at low m_X it is especially clear that gluon radiation cannot cure the flaws in the free b-quark decay picture: we know empirically that the gluonic degrees of freedom of QCD are frozen out at low mass. There are therefore no grounds for believing that the inclusion of gluonic degrees of freedom will significantly modify our basic conclusions regarding the electron end-point spectrum. Certainly, all the kinematic arguments against using the free-quark decay model apply with equal force to the radiative final states.

We have seen that in a limit in which pair creation is suppressed, the free b-quark decay model is likely to be valid in the usual (inclusive) QCD jet limit, but invalid near the high-energy electron end point. We next want to examine whether this conclusion can be expected to survive as we turn on pair creation (or leave the large-N_c limit). As a first step, motivated by the fact that at least most of the known low-lying mesons in which we are interested are narrow, we treat the amplitude for the production of dynamical pairs as a perturbation. It will then create, in lowest order, a small additional $qq\bar{q}\,\bar{q}$ piece in the previously pure $q\bar{q}$ meson state-vectors as well as a coupling between these stable eigenstates and the meson-meson continuum which will give them widths. The addition of widths to the stable bound states of our earlier picture presents no problems for our arguments: its main effect is to give an effective m_X spectrum which will more closely resemble the true resonance spectrum. In particular, this new effect does not dilute the argument against using the free-quark decay model at low m_X: it only suggests that the free-particle spectrum will "average the resonances" in a more direct way once the widths of the resonances become comparable to their spacings. There will be another effect of this presumed perturbation which cannot be viewed as a simple modification of our earlier picture. When the "four-quark" (i.e., $qq\bar{q}\,\bar{q}$) component of the $\bar{B}$ meson decays, the recoiling quark from $b \to q$ must be recombined in lowest order with a $\bar{q}\,\bar{q}q$ state. Part of the time this recombination will be into the four-quark component of X (e.g., for elastic scattering as $Q^2 \to 0$, each Fock-space component of the initial state scatters coherently into the final state), but it can also feed a *nonresonant* meson-meson continuum. This nonresonant continuum will also be a small perturbation on the resonance spectrum, to the extent that resonance widths can be treated as a small perturbation on the spectrum. Given the success of the narrow resonance approximation and of the valence-quark picture of mesons, it therefore seems unlikely that such nonresonant continua are very important.

Resonance dominance has, of course, been studied in inelastic lepton-nucleon scattering. The analogue to the action of our flavor-nonsinglet $b \to q$ current occurs in

nondiffractive lepton-nucleon scattering. (Diffractive scattering, which occurs when the virtual photon creates a quark-antiquark pair which then interacts with the nucleon, is not dominated by nucleon resonances in the final state. No analogous processes exist in B-meson decay, since the final state cannot contain a $b\bar{b}$ pair). Such nondiffractive scattering, which can be studied by examining nonsinglet structure functions, appears experimentally to be consistent with being saturated for $m \lesssim 2$ GeV/c^2 by the production of (overlapping) resonances with cross sections which rise and then fall with increasing momentum transfer with a scale of 1 GeV/c (Ref. 7).

In addition to such empirical checks of resonance dominance, nonresonant continuum production can also be studied theoretically. In the approximation in which quark pair creation is treated to lowest order, the resonant contribution to $\bar{B} \to X_1 X_2 e \bar{\nu}_e$ occurs when the action of the weak current is followed by pair creation, whilst nonresonant production occurs when pair creation acts before the current. Since both are controlled by the strength of the quark pair-creation operator, which is known from the study of meson decay (see, for example, Ref. 8), the continuum production can in principle be estimated.[9] In the absence of such estimates, and especially considering the evidence and arguments that nonresonant production will be small, it certainly seems worthwhile to predict, as we do here, the resonance *contributions* to semileptonic decay. This is *at least* the first step towards realizing a full sum over exclusive semileptonic decays.

Although we believe that our resonance dominance assumption for semileptonic decays will prove to be reasonably accurate, we should perhaps emphasize that if in some cases nonresonant processes are important, there is certainly no reason to expect the free-quark decay model to do a better job of describing them: apart from some small radiative corrections, the free-quark model also ignores the presence of extra quark-antiquark pairs in the B meson. On the other hand, the resonance model can at least partly take into account strong pair creation through its inclusion of resonance widths, whilst the free-quark decay model cannot. As an explicit example of this, consider the inclusive semileptonic spectra of $\bar{B}^0 = -b\bar{d}$ and $B^- = b\bar{u}$ decay from the $b \to u$ transition. In the free-quark decay model, ignoring isospin violation, these two spectra are identical, but in the resonance decay model they are different, as they should be. The point is that $b\bar{d} \to u\bar{d}$ whilst $b\bar{u} \to u\bar{u}$. The former transition thus creates a pure $I=1$ hadronic final state, whilst the latter has equal amplitudes to create $I=1$ and $I=0$. Since the $I=1$ and $I=0$ hadronic spectra differ, the two electron spectra will differ. To begin with, they have different thresholds: for $I=1$ it is $m_X \geq m_\pi$, but for $I=0$ we have $m_X > 2m_\pi$. The thresholds would only coincide, in the narrow resonance approximation, if the Okubo-Zweig-Iizuka (OZI) rule were exact so that $m_\pi = m_\eta$, $m_\rho = m_\omega$, etc. Even in this limit, the spectra would differ, as the widths of degenerate $I=1$ and $I=0$ mesons need not be the same since ordinary $m_s \neq m_u$ SU(3)-symmetry breaking can create width differences. One example we will encounter below occurs in the $J^{PC}=0^{++}$ mesons where, even in the OZI limit, $\Gamma_{I=1}/\Gamma_{I=0} \simeq \frac{1}{2}$. Thus, even without pair creation our resonance approximation would be no more "incomplete" than a free-quark decay calculation, and with resonance widths taken into account it clearly contains physics elements that the free-quark decay model cannot describe.

We warned the reader at the beginning of this Introduction that we would not be brief in delineating our reasons for doubting the validity of the free-quark decay model in the electron end-point region. We hope that even readers who were ready to accept this conclusion more easily will have appreciated seeing the case laid out in detail. We also expect that this discussion, whilst making it clear that our approach is in principle an improvement over the free-quark decay model, will have allowed the reader to anticipate that it still has many difficulties to overcome.

III. METHOD

We believe that the foregoing arguments convincingly demonstrate the need to replace the free-quark decay model for the end-point electron spectrum in semileptonic weak decays by an explicit summation over the spectra generated by exclusive channels. Unfortunately, it is easier to decide what needs to be done than to do it. Indeed, one of the other main conclusions of this and of our previous work[3,4] is that there are considerable theoretical uncertainties in carrying out this program, so that the extraction of accurate values or stringent limits on weak-mixing angles from such data will be correspondingly more difficult than was previously believed.

The problem, of course, is that there is no rigorous method available at the moment for handling the necessarily nonperturbative physics of the exclusive $\bar{B} \to X_c$ and $\bar{B} \to X_u$ transitions. One must therefore rely on a model for these states and, as the Introduction implies, we have chosen to rely on the constituent-quark model. This model is a phenomenological model of QCD in the nonperturbative regime, which has had considerable success in describing hadronic structure. It is especially well suited to (and well tested for) describing the low-lying resonances that contribute to the $\bar{B} \to X e \bar{\nu}_e$ end-point spectrum. Apart from sounding the warnings made above (and amplified below) regarding the inapplicability of the free-quark decay model to this problem, the other main purpose of this paper is to study this spectrum using the nonrelativistic quark potential model. Although we will discuss the uncertainties inherent in this calculation in some detail later (along with some possible improvements to the simple version of the model used here), we would like to state immediately that we will not be able to claim that our results are very reliable, especially for the crucial $\bar{B} \to X_u e \bar{\nu}_e$ transitions. On the other hand, for reasons that we hope are now obvious to the reader, we believe that a calculation of this type is essential if we are to be able to extract V_{bu}/V_{bc}, or a limit on it, from the data. Thus, although we will conclude that there are substantial uncertainties in our predictions, we will argue that they are a realistic reflection of the state of our understanding of nonperturbative QCD at the present time.

The transition matrix element for the process $\bar{B}^{0,-} \to X_q^{+,0} e \bar{\nu}_e$ is

$$T = \frac{G_F}{\sqrt{2}} V_{qb} \bar{u}_e \gamma_\mu (1-\gamma_5) v_{\nu_e} \langle X_q(p_X s_X) | j_{qb}^\mu | \bar{B}(p_B) \rangle \ , \tag{5}$$

where V_{qb} is the element of the Kobayashi-Maskawa matrix [formula (2)] which is appropriate for the $\bar{B} \to X_q$ transition, and j_{qb}^μ is the charged hadronic current in Eq. (1). Since the hadronic tensor

$$h_{\mu\nu} \equiv \sum_{s_X} \langle \bar{B}(p_B) | j_\nu^\dagger | X(p_X s_X) \rangle \langle X(p_X s_X) | j_\mu | \bar{B}(p_B) \rangle \tag{6}$$

must have the form

$$h_{\mu\nu} = -\alpha g_{\mu\nu} + \beta_{++}(p_B+p_X)_\mu (p_B+p_X)_\nu + \beta_{+-}(p_B+p_X)_\mu (p_B-p_X)_\nu + \beta_{-+}(p_B-p_X)_\mu (p_B+p_X)_\nu$$
$$+ \beta_{--}(p_B-p_X)_\mu (p_B-p_X)_\nu + i\gamma \epsilon_{\mu\nu\rho\sigma}(p_B+p_X)^\rho (p_B-p_X)^\sigma \ , \tag{7}$$

we can easily show, if the mass of the electron is neglected, that the differential decay rate of the $\bar{B}$ meson depends only on α, β_{++}, and γ, and is given by

$$\frac{d^2\Gamma}{dx\,dy} = |V_{qb}|^2 \frac{G_F^2 m_B^5}{32\pi^3} \left\{ \frac{\alpha}{m_B^2} y + 2\beta_{++} \left[2x \left[1 - \frac{m_X^2}{m_B^2} + y \right] - 4x^2 - y \right] - \gamma y \left[1 - \frac{m_X^2}{m_B^2} - 4x + y \right] \right\} , \tag{8}$$

where $x \equiv E_e/m_B$ and $y \equiv t/m_B^2 = (p_B - p_X)^2/m_B^2$. Of course Eq. (8) holds for other $M \to M' e^- \bar{\nu}_e$ decays with the appropriate substitutions; for decays to $e^+ \nu_e$ one must in addition reverse the sign of the term proportional to γ. The effects of resonance widths for the recoiling system X are discussed below and in Appendix D.

We will estimate α, β_{++}, and γ (for each channel X) using the quark model, building up the total electron spectrum $d\Gamma/dx$ by summing over contributing states X. If we include states X with mass up to m_X, we will then have the complete spectrum from the maximum value of x down to $x = \frac{1}{2}[1-(m_X^2/m_B^2)]$ so that this method, in contrast with a free-quark decay calculation, is potentially very suitable for studying the crucial end-point region of the spectrum.

Central to this calculation is, obviously, the possibility of reliably estimating the matrix elements $\langle X | j^\mu | \bar{B} \rangle$, and the inclusion of all relevant states which will contribute above some minimum E_e. Our first assumption, the rationale of which has already been discussed extensively in the Introduction, is that the sum over final hadronic states X will be approximately saturated by the ordinary quark-model resonances. This approximation thus ignores nonresonant production of multihadron states (for the reasons stated earlier) as well as gluonic excitations of mesons (meson hybrids). The latter approximation will be perfect down to values of E_e which correspond to the threshold for producing hybrids, and will become increasingly dubious at higher m_X, where the spectrum of such states is expected to become quite dense. (The excitation of these states is connected with the excitation of gluon radiation in the perturbative picture, but the connection is not a simple one.) This observation, along with the sheer complexity of extending the sum over X to high m_X, will mean that in practice we will truncate our calculation at some maximum m_X. To the extent that our truncation leaves out states, our results will then only apply above some minimum E_e.

A basic element of our method[10] is to make a correspondence between the Lorentz-invariant form factors f_i which occur as the coefficients of the various vectors X_i^μ that one can form from available kinematic variables in the expansion of the matrix element $\langle X(p_X s_X) | j^\mu(0) | \bar{B}(p_B) \rangle$ of the physical $\bar{B}$ and X, and those (which we call $\tilde{f}_i$) which appear in the quark-model calculation of $\langle \tilde{X}(\tilde{p}_X \tilde{s}_X) | j^\mu(0) | \tilde{\bar{B}}(\tilde{p}_B) \rangle$ [where, for example, $|\tilde{\bar{B}}(\tilde{p}_B)\rangle$ is the quark-model state vector in the weak-binding, nonrelativistic limit]. This "mock-meson method" (which is discussed more fully in Appendix A) is based on the observation that *in this limit* the quark-model state vectors form good representations of the Lorentz group, so that the f_i and $\tilde{f}_i$ are in one-to-one correspondence.

In our earlier work[3,4] we did not appreciate the full power of this method: we applied it only to form factors that were the coefficients of terms that were of zeroth or first order in the recoil momentum $\mathbf{p}_X$, believing that "higher-order" form factors, being of order v^2/c^2, were neither calculable nor important. The recent work of Altomari and Wolfenstein[5] demonstrated that the neglect of such form factors may not be justified. We have reexamined this issue, and have found that we can extend our calculation to include them. When we do so, we find that it was indeed a mistake to ignore them in general. The required extension of the method is discussed below and in Appendix A.

Although the accuracy of our form factors will obviously depend directly on the validity of the nonrelativistic quark model, it should be emphasized that this method not only makes our calculation fully relativistic kinematically, but also ensures that our calculated spectra respect all the correct physical thresholds occurring in these processes [that is, thresholds are all determined by Eq. (8) (or Appendix D) by observed masses and widths]. Moreover, since we expected, and find, rates for low-massed states that are dominated by soft recoils, our results will depend mainly on our ability to predict the form factors near zero recoil where the nonrelativistic quark model will be most reliable. In particular, we will find that in most cases rates are not very sensitive to the p_X^2 dependence of the f_i.

This is fortunate since within the weak-binding limit, where we know how to maintain Lorentz invariance, we can only compute the values of the form factors $\tilde{f}_i$ near zero recoil: the essence of the method is to identify f_i ($p_X^2 \simeq 0$) with $\tilde{f}_i$ ($\tilde{p}_X^{\,2} \simeq 0$). Indeed, the formulas we derive are only valid for wave functions with $\langle p_i^2 \rangle / m_i^2 \ll 1$ (p_i and m_i are the momentum and mass of quark i). We nevertheless follow the normal and reasonable quark-model phenomenology of using these formulas in the relevant regime where $\langle p^2 \rangle \sim \langle m_u^2 \rangle \sim \Lambda_{\rm QCD}^2$, i.e., of assuming that the weak-binding formulas can be extrapolated.

In general, we should expect such an extrapolation to be only qualitatively accurate. The fact that the quark model normally works somewhat better than this is presumably because its parameters have been adjusted to compensate for at least some of its deficiencies. There are, however, cases where quark-model calculations involve an overlap of wave functions that is near to unity, independent of details of the model. In these cases the quark potential model can be expected to be quite accurate. The transitions $\bar{B} \to X_c e \bar{\nu}_e$, in which the reduced masses of the quarks in the $\bar{B}$ and X_c are very similar, are examples of calculations which, at least in part, should exhibit such accuracy. At the opposite extreme is the accuracy we should expect from the quark model in its prediction of the large recoil behavior of form factors. A form factor will, in general, have an intercept at zero recoil which can be computed with typical quark-model accuracy. For p_X^2 small but nonzero, we will have

$$f_i(p_X^2) \simeq f_i(0) \left[1 - \left[\tfrac{1}{6} r_i^2 + \frac{a}{m^2} \right] p_X^2 \right] \tag{9}$$

in which we have allowed the slope of f_i to depend, as it might on dimensional grounds, on both the size of the hadrons (as represented by r_i) and on a quark mass m. (Such relativistic corrections of order p_X^2/m^2 are familiar from the hydrogen atom, where they give rise to the Darwin term correction to the Bohr spectrum.) In the weak-binding approximation $r_i^2 \sim 1/p^2 \gg m^{-2}$, so the p_X^2/m^2 term is lost, but in many hadrons of interest the two contributions to the slope of f_i could be comparable. Whilst irrelevant at $p_X^2 = 0$, this deficiency is potentially very serious at large p_X^2 where, for example, $\exp(-a p_X^2/m^2) \ll 1$. We will deal with this inadequacy of the nonrelativistic quark model below. First, we will give an explicit example of a calculation of the f_i using the mock-meson method.

Consider the matrix element for $\bar{B}^0 \to D^+$, where D^+ is the $c\bar{d}$ pseudoscalar ground-state meson. In general,

$$\langle D^+(p_D) | j_{cb}^{\mu} | \bar{B}(p_B) \rangle = f_+ (p_B + p_D)^{\mu} + f_- (p_B - p_D)^{\mu} , \tag{10}$$

where $f_\pm$ are Lorentz-invariant form factors which can be considered as functions of $t - t_m$, where $t_m = (m_B - m_D)^2$. (Note that in this example $\alpha = 0$, $\beta_{++} = |f_+|^2$, and $\gamma = 0$, so that in fact only the f_+ form factor is really required.) In the weak-binding, nonrelativistic limit, the matrix element of j_{cb}^{μ} between quark-model states $\tilde{\bar{B}}^0(\tilde{p}_B)$ and $\tilde{D}^+(\tilde{p}_D)$ [with, for example, $\tilde{m}_B = m_b + m_d$ so that $\tilde{E}_B = (\tilde{m}_B^{\,2} + \tilde{p}_B^{\,2})^{1/2}$] has an expansion exactly analogous to Eq. (10) with form factors $\tilde{f}_\pm$ that are functions of $\tilde{t} - \tilde{t}_m$.

The calculation of the form factor $\tilde{f}_\pm$ is straightforward. As explained in Appendix A, whilst such a calculation could be done using the full, properly normalized boosted state vectors of the weak-binding limit, it is more convenient to concentrate on special linear combinations of matrix elements which allow one to use simple nonrelativistic state vectors of the form

$$\left| \tilde{X}(\mathbf{p}_X s_X) \right\rangle = \sqrt{2\tilde{m}_X} \int d^3p \sum C^{s_x LS}_{m_L m_S} \phi_X(\mathbf{p})_{Lm_L} \chi^{Sm_S}_{s\bar{s}} \times \left| q \left[\frac{m_q}{\tilde{m}_X} \mathbf{p}_X + \mathbf{p}, s \right] \times \bar{q} \left[\frac{m_{\bar{q}}}{\tilde{m}_X} \mathbf{p}_X - \mathbf{p}, \bar{s} \right] \right\rangle \tag{11}$$

where $\chi^{Sm_S}_{s\bar{s}}$ couples the spins s and $\bar{s}$ to the total spin S, $\phi_X(\mathbf{p})_{Lm_L}$ is the $q\bar{q}$ relative momentum wave function, and the C factors couple L and S to the total angular momentum s_X. Assuming that the fields appearing in the currents create and destroy constituent quarks, we then simply compute free-quark matrix elements between states $\tilde{\bar{B}}$ and $\tilde{X}$ of the form of Eq. (11). In our example, we easily find that, for $\mathbf{p}_B = 0$ and $|\tilde{\mathbf{p}}_D| \ll \tilde{m}_D$,

$$(\tilde{m}_B + \tilde{m}_D)\tilde{f}_+ + (\tilde{m}_B - \tilde{m}_D)\tilde{f}_- = \sqrt{4\tilde{m}_B \tilde{m}_D} \int d^3p \, \phi_D^* \left[\mathbf{p} + \frac{m_d}{\tilde{m}_D} \tilde{\mathbf{p}}_D \right] \phi_B(\mathbf{p}) , \tag{12}$$

$$(\tilde{f}_+ - \tilde{f}_-)\tilde{\mathbf{p}}_D = \sqrt{4\tilde{m}_B \tilde{m}_D} \int d^3p \, \phi_D^* \left[\mathbf{p} + \frac{m_d}{\tilde{m}_D} \tilde{\mathbf{p}}_D \right] \phi_B(\mathbf{p}) \times \left[\frac{\mathbf{p}}{2m_b} + \frac{\mathbf{p} + \tilde{\mathbf{p}}_D}{2m_q} \right] . \tag{13}$$

These expressions, as already implied, neglect perturbative radiative corrections to the weak current. Although the weak current receives no infinite renormalizations, loop graphs give rise to corrections of the type $[\alpha_s(m_b)/\pi] \ln(m_b^2/\mu^2)$ coming from regions of integration where the loop momentum is smaller than m_b but larger than the typical momentum of the charm quark.[11] To proceed much further requires explicit momentum wave functions. We have chosen to use Schrödinger wave functions that are appropriate to the usual Coulomb plus linear potential

$$V(r) = -\frac{4\alpha_s}{3r} + c + br \tag{14}$$

with $\alpha_s = 0.5$, $c = -0.84$ GeV, and $b = 0.18$ GeV^2, and with constituent-quark masses $m_u = m_d = 0.33$ GeV/c^2, $m_s = 0.55$ GeV/c^2, $m_c = 1.82$ GeV/c^2, and $m_b = 5.12$ GeV/c^2. This simple model gives quite reasonable spin-averaged spectra of $u\bar{d}$, $c\bar{d}$, and $b\bar{d}$ mesons up to $L = 2$, and extends satisfactorily to the $c\bar{c}$ and $b\bar{b}$ systems (where we do not need it) with a running $\alpha_s = 0.4$ and 0.3, respectively. To avoid extensive numerical calculations, we

have used variational solutions of this Schrödinger problem based on harmonic-oscillator wave functions:

$$\psi^{1S}=\frac{\beta_S^{3/2}}{\pi^{3/4}}e^{-\beta_S^2 r^2/2}, \tag{15}$$

$$\psi_{11}^{1P}=-\frac{\beta_P^{5/2}}{\pi^{3/4}}r_+ e^{-\beta_P^2 r^2/2}, \tag{16}$$

$$\psi^{2S}=(\tfrac{2}{3})^{1/2}\frac{\beta_S^{7/2}}{\pi^{3/4}}(r^2-\tfrac{3}{2}\beta_S^{-2})e^{-\beta_S^2 r^2/2}, \tag{17}$$

in which the β's are employed as variational parameters. The resulting β values are given in Appendix C. With these wave functions we can perform analytically all the integrals we encounter. As described in Appendix C, we have checked the accuracy of these variational solutions and found them to be satisfactory. The analytic formulas for α, β_{++}, and γ, and the form factors f_i relevant to them, are given in Appendix B for all mesons X with $1S$, $1P$, and $2S$ spatial wave functions. These formulas, in conjunction with Eq. (8) and the physical masses and widths (taken from Refs. 12 and 13) of Table I, can be used to calculate $d^2\Gamma/dx\,dy$. (See Appendix D for the treatment of particle widths.)

Before this is done, however, we must face up to the expected inaccuracy of our nonrelativistic calculation of the p_X^2 dependence of form factors. Since all the mesons under explicit consideration here have roughly the same radius, we have dealt with this problem by allowing the computed slopes of all form factors to be modified by a common factor. This multiplicative constant is chosen to bring the calculated $F_\pi(Q^2)$ into better agreement with experiment in the low-Q^2 region, as shown in Fig. 1. [Charge radii are a special case of Eqs. (12) and (13).] This means that our computed form factors as functions of $t-t_m$ have all been replaced by the same functions of $(t-t_m)/\kappa^2$, where $\kappa=0.7$. We believe that this tampering with our calculation is justified by our earlier remarks, and that the modified form factors will give better estimates of semileptonic rates, but we will have to consider the uncertainties inherent in this procedure when we come to assess the reliability of our conclusions. Since, as previously emphasized, most decays are dominated by small recoils, we will find that most of our results are not very sensitive to κ. Unfortunately, the crucial $B\to X_u$ transitions will turn out to be the most sensitive to the behavior of the form factors away from the zero recoil point.

The study of exclusive semileptonic decays, of which our spectra are built, has a long history. This is especially true of the pseudoscalar-to-pseudoscalar transitions. The more recent work on exclusive charm and beauty semileptonic decays includes many different approaches. Initial work on heavy-quark semileptonic decay[15] was usually concentrated on the inclusive processes (the work of Ref. 2 traces it lineage back to these papers) but also gave rough estimates for exclusive decay rates. Later work tackled individual form factors employing quark-model ideas similar to ours,[16] infinite-momentum-frame quark models,[17] current-algebra ideas,[18] and other methods.[19] All studies prior to ours of which we are aware confined themselves to the explicit calculation of, at most, pseudoscalar-to-pseudoscalar and pseudoscalar-to-vector transitions; they generally agreed with each other (and with us) on the former and disagreed with each other (and with us) on the latter. Below, we will comment further on the comparison between our method and those of other authors.

IV. RESULTS

In this section we will present our results not only for B decay but also for related processes such as $K\to\pi e^-\bar{\nu}_e$ and $D\to Xe^+\nu_e$, since in addition to being interesting in their own right, in the cases where data exist they generally support the applicability of our methods. In later sections we will discuss the limitations of our results and the possibilities for improving them.

A. $K\to\pi e^-\bar{\nu}_e$

This process was previously studied[10] by the methods used here. We also find $f_+(t_m)\simeq 1.02$ and $f_-(t_m)\simeq -0.29$, both of which agree with experiment.

TABLE I. Physical masses and widths of the $1S$, $1P$, and $2S$ mesons. Masses and widths are taken from Ref. 12 if possible; properties of unobserved or controversial states (given in parentheses) are taken from Ref. 13. The entries in the table are, with all values in GeV: mass, width on resonance.

	$u\bar{d}$	$(\frac{1}{2})^{1/2}(u\bar{u}+d\bar{d})$	$s\bar{u}$	$c\bar{d}$	$b\bar{u}$
$1\,^1S_0$	0.14, 0.00	a	0.49, 0.00	1.87, 0.00	5.27, 0.00
$1\,^3S_1$	0.77, 0.15	0.78, 0.00	0.89, 0.05	2.01, 0.00	
$1\,^1P_1$	1.23, 0.15	1.19, 0.32	1.27, 0.09[b]	(2.44, 0.1)[b]	
$1\,^3P_2$	1.32, 0.11	1.27, 0.18	1.43, 0.10	(2.50, 0.1)	
$1\,^3P_1$	1.28, 0.32	1.28, 0.03	1.41, 0.18[b]	(2.49, 0.3)[b]	
$1\,^3P_0$	(1.09, 0.3)[c]	(1.09, 0.6)[c]	(1.24, 0.3)[c]	(2.40, 0.2)	
$2\,^1S_0$	1.30, 0.4[c]	(1.44, 0.1)[c]	(1.45, 0.2)[c]	(2.58, 0.3)	
$2\,^3S_1$	(1.45, 0.4)[c]	(1.46, 0.4)[c]	(1.58, 0.4)[c]	(2.64, 0.4)	

[a]We assume that the $(\frac{1}{2})^{1/2}(u\bar{u}+d\bar{d})$ strength is present with an amplitude of $(\frac{1}{2})^{1/2}$ in each of the $\eta(0.55)$ and $\eta'(0.96)$ corresponding to a mixing angle of approximately $-10°$.

[b] $^1P_1$-$^3P_1$ mixing has a negligible effect.

[c]The light-quark mesons in this sector are poorly understood. See the discussion in Ref. 13.

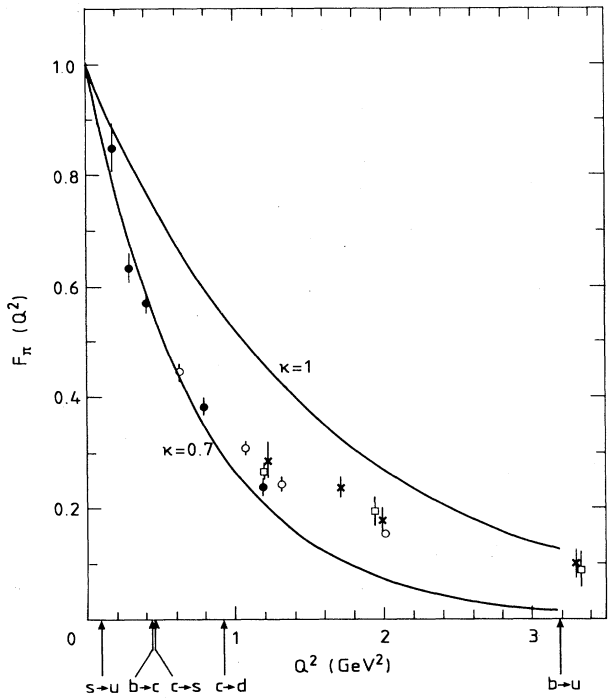

FIG. 1. Corrected ($\kappa=0.7$) and uncorrected ($\kappa=1.0$) pion form factor compared to experiment. The arrows along the abscissa show the Q^2 value corresponding to the maximum p_X reached by the indicated transition. For a compilation of the data, see Ref. 14.

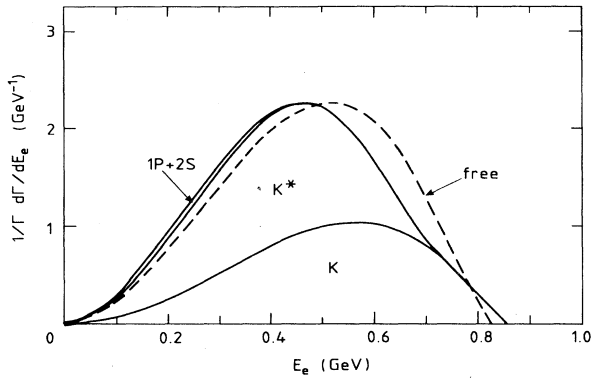

FIG. 2. $(1/\Gamma)(d\Gamma/dE_e)$ for $D\to X_s e^+\nu_e$ showing the contributions of K, K^*, and the total contribution from all $1S$, $1P$, and $2S$ states; also shown is the corresponding free quark curve. Absolute rates can be obtained by using $\Gamma=0.19\times10^{12}|V_{cs}|^2\,\mathrm{sec}^{-1}$ and $\Gamma^{\mathrm{free}}=0.35\times10^{12}|V_{cs}|^2\,\mathrm{sec}^{-1}$.

It is significant that we agree with the measured slope of the form factor f_+. When combined with the observations that we agree with the measured kaon charge radii and that the K wave function is already significantly different (on the scale set by the B wave function) from that of the π (see Appendix C), these results suggest that our use of the κ factor to take into account relativistic modifications of the form factors may be reasonably reliable. Finally, note that although SU(3) breaking in the quark masses is substantial, the Ademollo-Gatto theorem[20] protects f_+ from substantial deviations from unity. Equation (B8) for f_+ is not only consistent with the Ademollo-Gatto theorem; it also displays a shielding from flavor symmetry-breaking in the heavy-flavor case: $(1-f_+)$ is quadratic in $(m_b-m_q)/m_b$ for any light-quark mass m_d. Even for $B\to D$ we find that $f_+(t_m)$ differs from unity by only 20%.

B. $D\to Xe^+\nu_e$

All strange mesons X with mass $m_X<m_D$ can contribute to the electron spectrum for D-meson decay. Figure 2 shows our full predicted spectrum and how it is built up from contributing resonances. The free-quark decay spectrum is shown for comparison. Note that our spectrum is dominated by the two processes $D\to Ke^+\nu_e$ and $D\to K^*e^+\nu_e$, which we predict will constitute approximately 47% and 51% of the total, respectively. Although various experiments[21–23] agree that the K and K^* modes are dominant features of the m_X spectrum, it is still unclear whether they are as completely dominant as we predict: Ref. 23 finds a significant nonresonant $K\pi$ contribution. Despite this disagreement between experiments, there is agreement that the $K/(K+K^*)$ ratio is about 50%. Our $D\to K$ form factor is, moreover, once again in agreement with the measured form factor.[22] Using Ref. 24, we also predict the polarization of the K^*'s produced in $D\to K^*e\bar{\nu}_e$ to be $\Gamma(\text{longitudinal})/\Gamma(\text{transverse})=1.1$. Finally, we note that an *absolute* prediction for the total rate for semileptonic D decay is $\Gamma(D^0\to Xe^+\nu_e)=\Gamma(D^+\to Xe^+\nu_e)=0.19|V_{cs}|^2\times10^{12}$ sec^{-1}. Assuming that there are three generations of quarks, this is in reasonable agreement with the experimental result[1,22] of $(0.19\pm0.02)\times10^{12}$ sec^{-1}. Figure 3 shows our predicted electron spectrum, boosted as is appropriate for $D\bar{D}$ pairs produced from the $\psi(3770)$, compared with an experimental spectrum[21] of such electrons; we conclude that our model gives a reasonable account of these decays.[25] Figure 4 shows our predictions for the electron spectra from Cabibbo-suppressed D decays. The D^0 spectrum is dominated by the two processes $D^0\to\pi^-e^+\nu_e$ and $D^0\to\rho^-e^+\nu_e$, which constitute about 43% and 52% of the total, respectively.

Cabibbo-suppressed D^+ decay looks somewhat different, since in this case $X=\pi^0$, η, ρ^0, ω, . . . , in contrast with the free-quark decay model in which it is identical to D^0 decay. First of all, since

$$f_i(D_0\to\pi^+)=\sqrt{2}f_i(D^+\to\pi^0)\simeq2f_i(D^+\to\eta)\simeq2f_i(D^+\to\eta') \tag{18}$$

(assuming an η-η' mixing angle of approximately $-10°$), the fact that $m_\pi/m_D\ll m_{\eta'}/m_D$ leads to a rather different total pseudoscalar-meson contribution to the electron spectrum in D^+ decay versus D^0 decay. In addition, although given that with $m_\omega\simeq m_\rho$ the vector contribution to D^+ and D^0 decays would be equal in the stable resonance approximation, the fact that $\Gamma_\rho\gg\Gamma_\omega$ would lead to small differences in the vector contributions to the

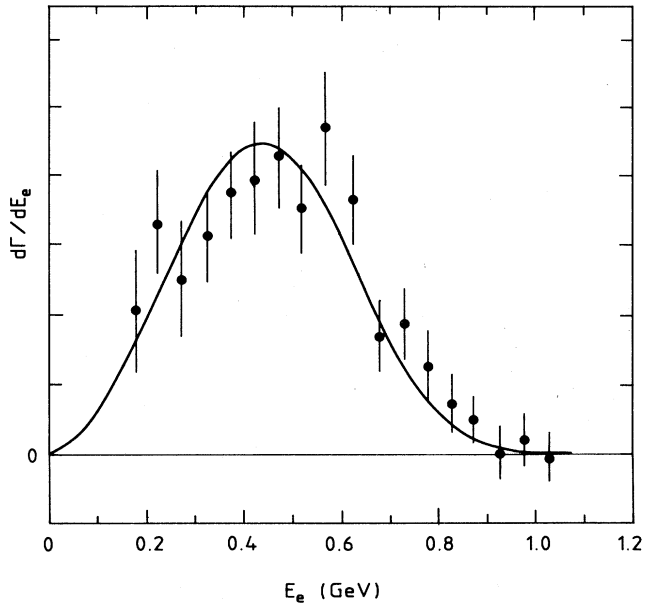

FIG. 3. $d\Gamma/dE_e$ for $D\to X_s e^+\nu_e$ from Fig. 2 boosted to correspond to D's from $\psi(3770)$ decay and compared to the data of Ref. 20. The integrated theoretical and experimental rates have been roughly adjusted to agree in order to facilitate a comparison of the spectral shapes. Note that these data contain a small contamination of $D\to X_d e^+\nu_e$.

D^+ and D^0 electron spectra; these differences are ignored in Figs. 4, but see Appendix D.

C. $\bar{B}\to Xe^-\bar{\nu}_e$

We now turn to the cases of interest for extracting $|V_{ub}|^2/|V_{cb}|^2$. We first discuss $\bar{B}\to X_c e^-\bar{\nu}_e$, where X_c is a charmed meson with mass $m_X<m_B$. Our present calculations extend only up to $m_X\simeq 2.5$ GeV/c^2, but as can be seen from Fig. 5, which shows how our predicted spectrum is built up out of contributing resonances, the full rate appears to be rapidly saturated by the lowest-lying states. We show the surprisingly similar shape of the free-quark decay spectrum for comparison. Our spectrum is once again dominated by the $1\,^1S_0$ and $1\,^3S_1$ states with the $D(1870)$ and $D^*(2020)$ contributing 27% and 60% (respectively) of our total spectrum.

Of the predictions made in this paper, we believe that those for $B\to De\bar{\nu}_e$ and $B\to D^*e\bar{\nu}_e$ are the most reliable. In the limit where the c- and b-quark masses are treated as large compared with the u- and d-quark masses, the form factors at threshold $t=t_m$ contain an overlap of wave functions that is unity, independent of the potential model. Also, in this limit the masses that appear in the form factors $f_+(t_m)$, $f(t_m)$, $g(t_m)$, and $a_+(t_m)$ are heavy-quark masses whose values are insensitive to the choice of potential model. The suppression of the form factors for $t\ll t_m$ arises because momentum must be transferred to the light quark in the recoiling $X=D$ or D^* state. However, if the momentum of X is $\mathbf{p}_X$, the

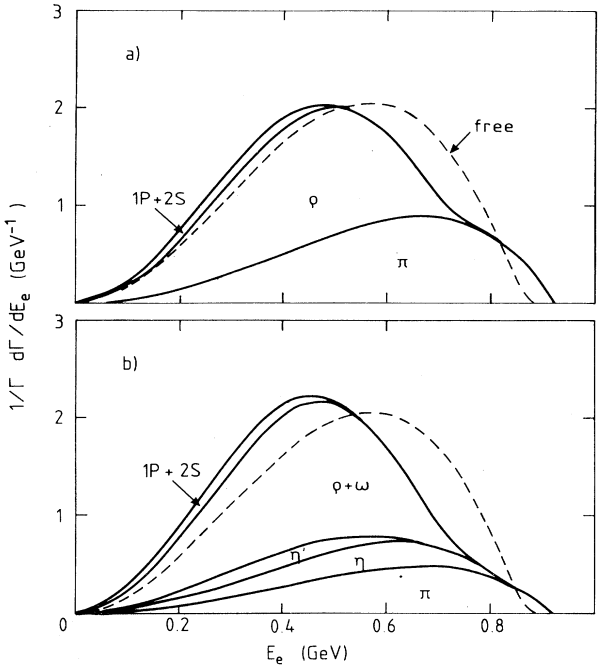

FIG. 4. (a) $(1/\Gamma)(d\Gamma/dE_e)$ for $D^0\to X_{\bar{d}}e^+\nu_e$ showing the contributions of π, ρ, and the total contribution from all $1S$, $1P$, and $2S$ states; also shown is the corresponding free quark curve. Absolute rates can be obtained by using $\Gamma=0.18\times10^{12}|V_{cd}|^2\,\mathrm{sec}^{-1}$ and $\Gamma^{\mathrm{free}}=0.54\times10^{12}|V_{cd}|^2\,\mathrm{sec}^{-1}$. Note that π and ρ constitute 43% and 52%, respectively, of the total rate. (b) $(1/\Gamma)(d\Gamma/dE_e)$ for $D^+\to X_d^0 e^+\nu_e$ showing the contributions of π, η, η', ρ, ω, and the total contribution from all $1S$, $1P$, and $2S$ states; also shown is the corresponding free quark curve. Absolute rates can be obtained by using $\Gamma=0.17\times10^{12}|V_{cd}|^2\,\mathrm{sec}^{-1}$ and $\Gamma^{\mathrm{free}}=0.54\times10^{12}|V_{cd}|^2\,\mathrm{sec}^{-1}$. Note that $\Gamma(D^+\to X_d^0 e^+\nu_e)/\Gamma(D^0\to X_d^- e^+\nu_e)=0.93$ mainly from the effects of the η and η' channels which are especially evident at the highest E_e, and that π, η, η', ρ, and ω constitute, respectively, 23%, 12%, 5%, 28%, and 27% of the total rate.

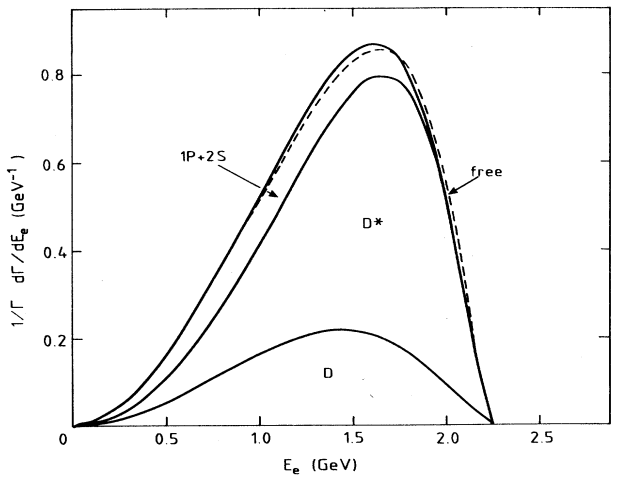

FIG. 5. $(1/\Gamma)(d\Gamma/dE_e)$ for $B\to X_c e^-\bar{\nu}_e$ showing the contributions of D, D^*, and the total contribution from all $1S$, $1P$, and $2S$ states; also shown as a dashed curve is the corresponding free quark curve. Absolute rates can be obtained by using $\Gamma=0.41\times10^{14}|V_{cb}|^2\,\mathrm{sec}^{-1}$ and $\Gamma^{\mathrm{free}}=0.49\times10^{14}|V_{cb}|^2\,\mathrm{sec}^{-1}$.

light quark only carries momentum $[m_d/(m_c+m_d)]\mathbf{p}_X$. The presence of the heavy c quark thus causes the form factors to vary only a little over the available phase space.

Our D^* branching fraction of 0.60 is consistent with the preliminary measurements[1] of 0.8 ± 0.3. It should be noted that the rate for $B\to D^* e\bar{\nu}_e$ is determined by three form factors: f, g, and a_+. The dependence on f, g, and a_+ can be partially separated[24,26] by observing the polarizations of the D^*'s produced in $B\to D^* e\bar{\nu}_e$. The production rate of transversely polarized D^*'s is independent of a_+, whilst the production rate of longitudinally polarized D^*'s does depend on a_+. We predict $fa_+(t_m)=-1.00$, which gives roughly equal amounts of longitudinally and transversely polarized D^*'s. As $fa_+(t_m)$ is increased, the rate for longitudinally polarized D^*'s increases. For example, at $fa_+(t_m)=0$, $D^*(\text{longitudinal})/D^*(\text{transverse})\simeq 2$. A recent measurement[27] of the D^* polarization is consistent with the D^*'s in semileptonic B decay being purely longitudinal. Further measurements of this polarization are needed as such a situation may be difficult to reconcile with not only calculations of the type presented here, but also the free-quark decay model. (In this model one can predict inclusive probabilities for the production of hadronic systems recoiling with helicities ±1 and 0 by using the fact that the initial state has zero angular momentum so the hadronic helicity must balance that of the $e\bar{\nu}_e$ system.)

Anticipating that $b\to u$ / $b\to c$ will be small, our absolute prediction for the total B semileptonic rate is

$$\Gamma(\bar{B}^0\to X^+e^-\bar{\nu}_e)=\Gamma(\bar{B}^-\to X^0e^-\bar{\nu}_e)=0.41\times10^{14}|V_{cb}|^2\ \text{sec}^{-1}\ . \quad (19)$$

From the experimental value of this rate[12,28–30] we find that

$$|V_{cb}|=0.048\pm0.005\pm0.006\ . \quad (20)$$

Below, we will discuss the uncertainties in this determination of $|V_{cb}|$ associated with our calculation [the second error in Eq. (20); the first is experimental and arises from uncertainties in the B lifetime and semileptonic branching ratio].

Figure 6 shows our predicted spectrum for $\bar{B}^0\to X_u^+e\bar{\nu}_e$, where X_u^+ is a $u\bar{d}$ meson belonging to any of our eight lowest-lying meson families. It is clear that the $1S$, $1P$, and $2S$ states (which include all states with $m_X\lesssim 1.7\ \text{GeV}/c^2$) do not in this case saturate the rate. Recall, however, that our calculation does saturate the contributions of $\bar{B}\to X_u e\bar{\nu}_e$ in a region at the end of the spectrum where $\bar{B}\to X_c e\bar{\nu}_e$ vanishes. This fraction of the spectrum is therefore all we need for determining (or for setting an upper limit on) $|V_{ub}|$. Note that our $B\to X_u$ spectrum is considerably softer than the free-quark spectrum.

In the Introduction it is clearly indicated why $b\to u$ might not be saturated by these lowest-lying states, in contrast with the other transitions we discuss. Recall that (ignoring relative momentum in the decaying B) free-quark decay populates recoiling masses m_X in the range from m_q+m_d up to $[(m_q+m_d)^2+(m_d/m_b)(m_b-m_q)^2]^{1/2}$ and that this range (0.02 GeV/c^2 for $s\to u$, 0.15 GeV/c^2 for $c\to s$, 0.26 GeV/c^2 for $c\to u$, 0.16 GeV/c^2 for $b\to c$, and 0.72 GeV/c^2 for $b\to u$) is considerably smaller than the typical orbital excitation energy of 0.5 GeV in every case except that of $b\to u$, where it is actually greater. (A more realistic estimate, taking into account the mean momentum in the B wave function, gives a range in $b\to u$ of more than 1 GeV/c^2.) It is therefore not at all surprising that there are, for example, significant $2S$ components in the $b\to u$ spectrum; nor should we be surprised that our truncated calculation is incomplete. We have nevertheless checked this point explicitly by extending our calculation for pseudoscalar mesons to higher masses by computing $\bar{B}^0\to\pi(nS)e\bar{\nu}_e$, where $\pi(nS)$ is the nth pion state. A description of the calculation is given in Appendix C; Fig. 7 displays the results, which exhibit the convergence conjectured in Refs. 3 and 4. Note that the $1S$ and $2S$ levels already give about two-thirds of the total pseudoscalar contribution, suggesting that a complete calculation would converge, as described in the Introduction, to a $d\Gamma/dE_e$ comparable to the free-quark rate at low E_e.

Since our end-point spectrum is considerably softer than the free-quark decay electron spectrum, we expect that a complete sum over final states X_u would lead to a total semileptonic decay rate that is somewhat smaller than the corresponding free-quark rate. It should be recalled, however, that the $b\to u$ free-quark rate [see Eq. (4)] it itself quite uncertain, since the effective value of m_b entering in this equation is not well known.

To extract a value (or limit) for V_{ub} using our predicted

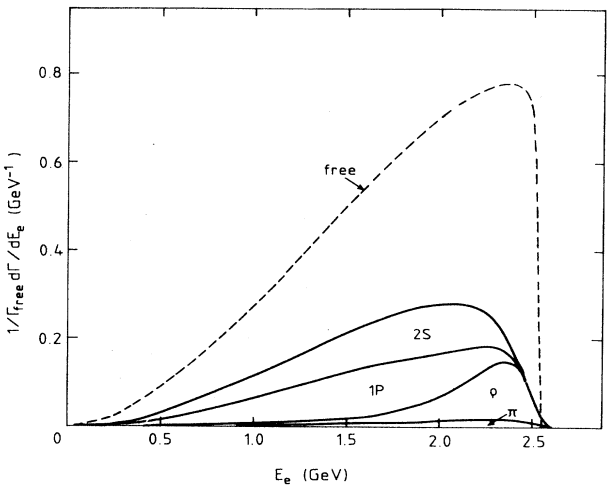

FIG. 6. $(1/\Gamma^{\text{free}})(d\Gamma/dE_e)$ for $B\to X_u^+e^-\bar{\nu}_e$ showing the contributions of π, ρ, the $1P$ states, and the $2S$ states π' and ρ'; also shown as a dashed line is the free quark curve $(1/\Gamma^{\text{free}})(d\Gamma^{\text{free}}/dE_e)$. Absolute rates can be obtained by using $\Gamma^{\text{free}}=1.18\times10^{14}|V_{ub}|^2\ \text{sec}^{-1}$. The partial rates to exclusive channels, in units of $10^{14}|V_{ub}|^2\,\text{sec}^{-1}$ are $\Gamma(B\to\pi(1S))=0.021$, $\Gamma(B\to\rho(1S))=0.083$, $\Gamma(B\to{}^3P_2)=0.007$, $\Gamma(B\to{}^3P_1)=0.093$, $\Gamma(B\to{}^3P_0)=0.007$, $(\Gamma B\to{}^1P_1)=0.059$, $\Gamma(B\to\pi(2S))=0.110$, and $\Gamma(B\to\rho(2S))=0.053$. Thus the $1S$, $1P$, and $2S$ states computed account for a rate of $0.43\times10^{14}|V_{ub}|^2\,\text{sec}^{-1}$.

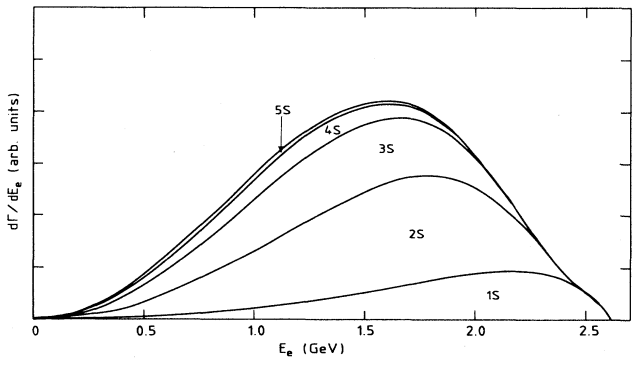

FIG. 7. $(d\Gamma/dE_e)$ for $\bar{B}^0 \to \pi^+(nS)e^-\bar{\nu}_e$ showing convergence of the sum over exclusive pseudoscalar channels. In units of $10^{14}|V_{ub}|^2\,\mathrm{sec}^{-1}$ the individual rates to $\pi(1S)$, $\pi(2S)$, $\pi(3S)$, $\pi(4S)$, and $\pi(5S)$ are 0.031, 0.077, 0.047, 0.014, and 0.003, respectively. See the discussion of Appendix C for the relation of these rates to those of Fig. 6.

electron spectra, they must first be boosted as appropriate for $B\bar{B}$ pairs produced on the $\Upsilon(10580)$ and then smeared with experimental resolutions. For such analyses based on the earlier version[3,4] of our model (we expect very similar conclusions will emerge from this version), see Refs. 31–33 which showed that our pure $b \to c$ spectrum gave a satisfactory fit to the data and derived corresponding limits on V_{ub}. In Sec. V we will discuss the reliability of such limits.

V. DISCUSSION

Most early attempts to extract $|V_{ub}|^2/|V_{cb}|^2$ from the $\bar{B} \to Xe\bar{\nu}$ end-point spectrum used Eq. (3), with $d\hat{\Gamma}$'s given by a QCD-perturbed free-quark calculation in which extra parameters were introduced to correct for nonperturbative effects.[2] With recent improvements in the data, these attempts have, as might have been anticipated, encountered some difficulties.[1] These difficulties have made it clear that the predicted end-point behavior of the calculations of Ref. 2 are being controlled to a large extent by parameters introduced to describe bound-state effects, and not by perturbative QCD. Our calculation, in contrast, is more suitable for the end-point region: it correctly handles the kinematics of the opening of new channels with their appropriate quantum numbers; also, the dynamics of the quark model is more appropriate to this region.

Our calculations still have serious sources of uncertainty. Nevertheless, we would first like to stress that our calculation of $\bar{B} \to X_c e\bar{\nu}_e$ seems to be immune to most of these uncertainties. The success of the analogous $D \to X_s e^+ \nu_e$ calculation is evidence of the reliability of $\bar{B} \to X_c e\bar{\nu}_e$, but we have also checked that reasonable variations of the wave functions (for example, ones that change κ by 30%) have little effect on our spectra.

In the foregoing we have discussed the reasons for the stability of our $\bar{B} \to X_c$ results. It is more difficult to assess the systematic uncertainties associated with this calculation. We will discuss below some possible improvements to our methods which could check several possible sources of error, but for now we just note that the success of our predictions for $K \to \pi$, $D \to X_s$, and various known features of $\bar{B} \to X_c$, along with the demonstrably weak parameter dependence of our results, lead us to have confidence that the absolute-rate predictions shown in Fig. 5 are valid at the 20% level, and that the shape of the predicted electron spectrum is very good.

For $\bar{B} \to X_u e\bar{\nu}_e$ our predicted spectral shape is once again stable in the end-point region. However, in this case we have considerably less confidence in our ability to predict absolute rates: few of the features which stabilized $B \to X_c e\bar{\nu}_e$ are present here. For example, when we vary the β's and κ over the ranges that we consider reasonable, we get substantial variations in the absolute rates of the exclusive modes. We have concluded that our absolute-rate predictions could be as much as 30% higher and a factor of 2 lower than the true rates. This uncertainty will affect our ability to determine (or bound) V_{ub} from the data.

The model sensitivity of our $\bar{B} \to X_u e\bar{\nu}_e$ results is not unrelated to the slow convergence of the summation over X_u. As discussed in the Introduction, in a heavy-quark decay, once E_e is small enough for all relevant thresholds to have been crossed, the summation should converge to the free-quark spectrum *independent of the details of the confinement dynamics.* However, the way this spectrum is split up into exclusive channels will depend on these details and will naturally become more difficult to calculate as the strength becomes divided into more channels. Since the end-point spectrum corresponds to the high-E_e tail of a few of these states, it is correspondingly more difficult to compute.

As already mentioned in Sec. III, there is no other calculation of exclusive semileptonic decay matrix elements known to us which is as extensive as this one. Nevertheless, in looking for possible improvements to our method, it may be useful to make a comparison with some other existing calculations.[16–19]

Reference 16 consists of calculations that are very similar in spirit to ours, and when they overlap with us they seem to differ mainly on matters of detail (although we are unable to reproduce some of the results quoted in these papers). The best method for connecting results such as ours with experiment will, it seems to us, depend on a close interplay between experiment and this still-developing phenomenology (see Sec. VI for further discussion). The works listed in Ref. 18 exploit some potentially very powerful constraints on weak matrix elements arising from low-energy theorems. It could be very useful to try to impose these constraints on our calculation. (Low-energy theorems also limit the importance of channels containing additional soft pions. These constraints might be exploited to study theoretically the possible importance of the nonresonant processes discussed in Sec. II.) However, low-energy theorems are clearly limited in scope and cannot be expected to give as complete a picture of the weak matrix elements as would a full dynamical model. In our opinion, the method of Ref. 17 is the one most likely to provide, at some future time, an alter-

native to ours. However, at the moment we see several difficulties for this method: (i) It is based on infinite-momentum-frame wave functions (or light-front wave functions) about which we know very little either theoretically or phenomenologically. Thus, unlike the quark potential model, this phenomenology is not yet "tuned." (ii) Matrix elements are calculated at $t=0$ and then extrapolated to $t=t_m$ by invoking pole dominance. As we have stressed, t_m (corresponding to zero recoil) is the point where form factors for transitions to low-lying states will tend to peak. A calculation at $t=0$ therefore calculates the form factors where they are small and extrapolates them to where they are large. Here the difficulty is compounded by the fact that a $t=0$ calculation requires knowledge of the infinite-momentum-frame wave functions near their end points where they are small and least well understood. We will also argue below that the use of pole-model form factors is not generally appropriate and may not be justified in transitions such as $B\to X_u$. (iii) While the potential advantages of a relativistic formalism will be obvious from the difficulties we encountered in our work, there are some serious obstacles to making such a formalism consistent. In particular, infinite-momentum-frame wave functions cannot be constructed to be good eigenstates of J^P (except in the weak-binding limit in which this formalism becomes equivalent to ours); good J^P states could be obtained in general only by solving the equation of motion, which is at present impossible.

We might hope to reduce the uncertainties in the results we have presented by improving upon our quark-model calculation. To a certain extent we believe that this is possible. It would be useful, for example, to extend our calculations to higher masses (see, however, the warning in Sec. II). It would also be interesting to check on the importance of relativistic effects. We have just commented on one possible way of doing so. We have some doubts about the utility of making a check of such effects in the bag model (although it naturally comes to mind as a relativistic quark model), since one will encounter two problems with the static bag approximation: heavy-quark wave functions will not be adequately described, and the recoiling quark will populate both excited-meson states and spurious center-of-mass motion states. An alternative is to build some relativistic corrections into the quark-potential model. Here one must be careful to ensure that the model predicts meson spectra and static properties as well as the nonrelativistic quark model. (Note that the models of Refs. 10 and 13, which are of this type, predict that the discrepancy between the data and the nonrelativistic quark-model prediction for G_A/G_V in neutron decay will be reduced by a factor of $m_d^2/m_b m_q$ in, for example, the f form factor in $\bar{B}\to D^*$ decays.) We might also consider supplementing our quark-model calculation with some sort of pole-dominance model for the t dependence of the weak form factors (this is the usual method in Refs. 16–19). Our form factors are actually quite close to pole-dominance form factors in many cases, but from our calculation we can also appreciate that the pole model is not generally applicable. These form factors are largest (and therefore normally most important) at the zero recoil point where the quark model applies and where, in some cases, there is no reason to expect a single meson pole to dominate. An extreme case would be the elastic form factor of the η_c: this form factor near $t=0$ will clearly be controlled by the η_c wave function [which will give $r_f\sim(m_c\alpha_s)^{-1}$] and not by the lowest vector meson (which would give $r_f\sim m_c^{-1}$). The failure of vector-meson dominance is in this case easy to understand: on the scale of m_ψ^2, the spacing between vector-meson states is small. It is also dubious whether the pole model applies to transitions such as $\bar{B}\to X_u$. In such a transition, t can vary from zero to $t_m=(m_B-m_\pi)^2$, whilst the spacing between B^* poles is of order $(300\ \mathrm{MeV})^2$ making it very difficult to understand why a simple pole model should work. Of course for light-quark states our form factors also have difficulties, as discussed in Sec. II. This is illustrated in Fig. 1 which shows the measured pion electromagnetic form factor $F_\pi(Q^2)$ and our quark-model prediction for it. With the factor κ the two agree out to about $Q^2=1$ GeV^2. Beyond this point (a region relevant only in the $b\to u$ transition) our exponential form factor falls below the measured one. (This deficiency and our neglect of nonresonant contributions tends to make limits on $|V_{bu}|$, obtained from a comparison of our results with experimental data on the end point of the electron spectrum, conservative ones, and is partly responsible for the lopsided theoretical errors on our predicted rate for $\bar{B}\to X_u e\bar{\nu}_e$ mentioned earlier.)

As stated previously, we can also improve upon this calculation by including resonance widths and estimating nonresonant production. Figure 8 shows the effect on the contribution of the f_0 (the $I=0$, $^3P_0$ $q\bar{q}$ state) to the $\bar{B}\to X_u e\bar{\nu}_e$ electron spectrum. Even for a broad resonance (which, incidentally makes up only a few percent of the total $\bar{B}\to X_u e\bar{\nu}_e$ rate) the width does not lead to a significant increase in the rate in the end-point region $E_e>2.3$ GeV, where $\bar{B}\to X_c e\bar{\nu}_e$ is kinematically forbidden.

VI. CONCLUSIONS AND SUMMARY

We have argued that the extraction of $|V_{ub}|^2/|V_{cb}|^2$ from the end point of $\bar{B}\to Xe\bar{\nu}_e$ requires an understanding of the nonperturbative physics which binds the quarks into hadrons. The quark-model calculation presented here represents one approach to this physics. Although it suffers from considerable uncertainties, we believe that these are typical of the uncertainties at present associated with our ability to predict when nonperturbative strong interactions are important.

Our results give a $\bar{B}\to X_c$ end-point spectrum that is slightly softer than the free-quark spectrum; this spectrum fits the data quite well with no admixture of $\bar{B}\to X_u$. Our $\bar{B}\to X_u$ spectrum is considerably softer than the free-quark spectrum, so that the limits that can be obtained on the strength of V_{ub} from the lepton spectra in the end-point region will be correspondingly weaker.

Although improved measurements of the end-point spectrum may well remain the best way to limit and even-

tually observe V_{ub}, our calculation does open up one other possible avenue. Since we provide absolute rates for a large number of *exclusive* semileptonic modes of decay to noncharmed mesons, a limit on (or a measurement of) any of these modes can now be turned into a limit on (or a measurement of) $|V_{ub}|$.

We also note that, as a by-product of these calculations, we have predicted how the $B\to X_c$, $B\to X_u$, $D\to X_s$, and $D\to X_d$ spectra are built up out of exclusive channels. These predictions, which are of interest in their own right, can be used to check the reliability of our calculations. It would be especially rigorous to check our predictions (through α, β_{++}, and γ) of the detailed structure of the relevant Dalitz plots. Another possible application of our results is to check the validity of the KM parametrization of the mixings. For example, using our absolute predictions for the total rate for semileptonic D decay we deduce that $|V_{cs}|=(1.00\pm0.05\pm0.10)$, where the first error is experimental and the second is the estimated error in our prediction of the semileptonic D-decay rate. We could also use our predictions to extract V_{cd} from an exclusive mode such as $D^+\to\rho^0 e^+\nu_e$. Indeed, in the short term it is perhaps only by checking detailed predictions such as these for various exclusive channels that we can assess the reliability of our predictions and eventually improve our ability to calculate weak matrix elements. Eventually, of course, such matrix elements will be accurately calculated on the lattice. Once this can be done, it will be possible to convert the increasingly sophisticated measurements of exclusive semileptonic decays directly into accurate measurements of the Kobayashi-Maskawa angles.

ACKNOWLEDGMENTS

This research was supported in part by grants from the Natural Sciences and Engineering Research Council of Canada and by DOE Grants under Contracts Nos. DEAC-03-91-ER40050, DEA CO3-81-ER40051, and DE-FG03-84ER40172. M.B.W. also was supported by the Alfred P. Sloan Foundation. N.I. gratefully acknowledges the hospitality of the Department of Theoretical Physics at Oxford and of the Theoretical Physics Division at CERN where this work was completed. B.G. acknowledges the Tolman Foundation for Financial support.

APPENDIX A: THE "MOCK-MESON" METHOD

As discussed briefly in the text, the "mock-meson" method is based on an expansion

$$\langle B|j^\mu(0)|A\rangle=\sum_i f_i(t-t_m)X_i^\mu\ , \tag{A1}$$

where the X_i^μ are Lorentz vectors constructed from the available kinematic variables, and the f_i are Lorentz-invariant form factors which may depend on $t=(p_B-p_A)^2$, t_m being the maximum four-momentum transfer $(m_B-m_A)^2$. In the weak-binding limit, as we will see below, one can construct nonrelativistic quark-model states which are good representations of the Lorentz group, so that

$$\langle \tilde{B}|j^\mu(0)|\tilde{A}\rangle=\sum_i \tilde{f}_i(\tilde{t}-\tilde{t}_m)\tilde{X}_i^\mu\ , \tag{A2}$$

where $\tilde{A}$ is the quark-model state ("mock meson") corresponding to the hadron A, etc., and where there is therefore a one-to-one correspondence between the f_i and the $\tilde{f}_i$. Since, as we will see shortly, Eq. (A2) applies exactly only in the limit of zero binding, where the matrix element has support solely at zero recoil, this correspondence can only be used to identify f_i and $\tilde{f}_i$ at zero recoil. Relationships away from zero recoil, for example, slopes, will in general not be Lorentz invariant by terms of order p_i^2/m_i^2, where p_i and m_i are constituent three-momenta and masses. The problems this entails, given that the actual quark-model wave functions for hadrons containing light quarks have p_i comparable to m_i, are discussed in the text.

Before giving any details, we would like to describe qualitatively, and briefly, why it is that the nonrelativistic quark model can predict all the f_i, including those that are coefficients of X_i^μ that are of higher order than v/c in recoil velocity. We will take as our example the first matrix element needed here where this issue arises: $\langle V(\mathbf{p}_X s_X)|A^\mu(0)|\bar{B}(\mathbf{p}_B)\rangle$. As shown in Appendix B, this matrix element is described by three form factors, and we can easily see that one linear combination of the three form factors can be determined at order $(v/c)^0$ and one at order v/c, but that the third linear combination requires a calculation to order $(v/c)^2$. To see why this is possible, it is convenient to consider $\langle\bar{B}(\mathbf{p}_B)|A^\mu(0)|V(\mathbf{0},s_X)\rangle$ (which we know has the same information in it by Lorentz invariance), since we can then identify the three Lorentz-invariant form factors with three partial-wave amplitudes: $A^0(0)$ is a pseudoscalar operator and, when applied to the vector $|V(\mathbf{0},s_X)\rangle$, gives a $J^P=1^+$ state which must therefore produce $|B(\mathbf{p}_B)\rangle$ recoiling in a P wave. $\mathbf{A}(0)$ on $|V(\mathbf{0},s_X)\rangle$ can give quantum numbers $J^P=2^-,1^-,0^-$, but only 2^- and 0^- can be reached by the recoiling B, which will be in a D wave and S wave for 2^- and 0^-, respectively. These S-, P-, and D-wave amplitudes are of course required by nonrelativistic kinematics to behave like $(v/c)^0$, v/c, and $(v/c)^2$, respectively, and can be related to the three Lorentz-invariant amplitudes. Since there is nothing intrinsically relativistic about recoiling in a D wave, we see that in principle this amplitude can be calculated nonrelativistically. Indeed, if one takes care to isolate a given partial wave in the matrix element, ordinary quark-model state vectors can be used for all three form factors.

Such a calculation will not be Lorentz invariant to order $(v/c)^2$ [in the sense that with ordinary quark-model state vectors, relationships between different components of the matrix element with various spin states and various values of $\mathbf{p}_B$ and $\mathbf{p}_X$ will not be correct to order $(v/c)^2$], but it will give the zero recoil value of the three form factors. Alternatively, one can calculate with the full state vectors given below, which ensure exact Lorentz invariance in the weak-binding limit.

The construction of quark-model states that are representations of the Lorentz group in the weak-binding limit

begins with the construction of a free quark-antiquark "momentum shell" state in its center-of-mass frame, with definite J^P and definite relative momentum p. The usual quark-model states are superpositions of such states weighted with a wave function that depends on p. However, for fixed p, such states could be boosted with a free-particle boost under which they would form representations of the Lorentz group with mass $M=(p^2+m_q^2)^{1/2}+(p^2+m_{\bar{q}}^2)^{1/2}$, spin J, and momentum $\mathbf{p}=\gamma\mathbf{v}M$, where $\mathbf{v}$ is the boost velocity and $\gamma=(1-v^2/c^2)^{-1/2}$. Since a superposition of such free-particle rest-frame states has masses in a range δM, it cannot be trivially boosted to form a representation of the Lorentz group. In an interacting theory, such a superposition might be a state of definite mass, but then its boost operator is nontrivial. However, a superposition over a very narrow range of momenta will, under a free-particle boost, form an approximate representation of the Lorentz group. Weak binding is a particular example of such a case in which we can expect deviations from Lorentz invariance to vanish as $\langle p^2\rangle\to 0$.

To apply this method, one could therefore construct exact representations of the Lorentz group with fixed p, and then superpose them. With normalizations

$$\langle q(\mathbf{p}'s')|q(\mathbf{p}s)\rangle=\frac{E}{m}\delta_{s's}\delta^3(\mathbf{p}'-\mathbf{p}) \tag{A3}$$

for quarks and antiquarks and

$$\langle M(\mathbf{p}'s')|M(\mathbf{p}s)\rangle=2E\delta_{s's}\delta^3(\mathbf{p}'-\mathbf{p}) \tag{A4}$$

for mesons, one would get the result

$$|X(p_X s_X)\rangle=\sqrt{2\tilde{m}_X}\int d^3p\sum C^{s_X LS}_{m_L m_S}\phi_X(\mathbf{p})_{Lm_L}\chi^{Sm_S}_{s\bar{s}}(\mathbf{p},\mathbf{p}_X)|q(\mathbf{L}_q(\mathbf{p},\mathbf{p}_X),s)\bar{q}(\mathbf{L}_{\bar{q}}(-\mathbf{p},\mathbf{p}_X),\bar{s})\rangle \tag{A5}$$

in which everything is as in Eq. (11) except that now $\mathbf{L}_i(\mathbf{p},\mathbf{p}_X)$ is the momentum of a particle of mass m_i and momentum $\mathbf{p}$, boosted by the Lorentz transformation that takes X with mass $\tilde{m}_X$ to momentum $\mathbf{p}_X$, and

$$\chi^{Sm_S}_{s\bar{s}}(\mathbf{p},\mathbf{p}_X)=N_{ss'}(\mathbf{p},\mathbf{p}_X)\bar{N}_{\bar{s}\bar{s}'}(\mathbf{p},\mathbf{p}_X)\chi^{Sm_S}_{s'\bar{s}'} \tag{A6}$$

where $\chi^{Sm_S}_{s'\bar{s}'}$ are the usual Clebsch-Gordan coefficients that couple s' and $\bar{s}'$ to Sm_S, and where with $E_q=(m_q^2+p^2)^{1/2}$, $E_{\bar{q}}=(m_{\bar{q}}^2+p^2)^{1/2}$, and $\mathbf{p}_X=\gamma v\tilde{m}_X\hat{\mathbf{z}}$,

$$N^q_{++}=N^q_{--}=[(1+\gamma)(E_q+m_q)+v\gamma p_z]/D_q\ , \tag{A7}$$

$$N^q_{-+}=-N^{q*}_{+-}=-\gamma v p_+/D_q\ , \tag{A8}$$

with $D_q=\{2(1+\gamma)(E_q+m_q)[\gamma(E_q+vp_z)+m_q]\}^{1/2}$ and

$$\bar{N}^{\bar{q}}_{++}=\bar{N}^{\bar{q}}_{--}=[(1+\gamma)(E_{\bar{q}}+m_{\bar{q}})-v\gamma p_z]/\bar{D}_{\bar{q}}\ , \tag{A9}$$

$$\bar{N}^{\bar{q}}_{-+}=-\bar{N}^{\bar{q}*}_{+-}=-\gamma v p_+/\bar{D}_{\bar{q}}\ , \tag{A10}$$

with $\bar{D}_{\bar{q}}=\{2(1+\gamma)(E_{\bar{q}}+m_{\bar{q}})[\gamma(E_{\bar{q}}-vp_z)+m_{\bar{q}}]\}^{1/2}$. In the weak-binding limit it is easily seen that (A5) reduces to Eq. (11) of the text.

Fortunately, as the discussion at the beginning of this appendix suggests, in many cases (including all those of interest here) one need not be so careful since nonrelativistic physics determines the zero recoil behavior of the $\bar{f}_i$. The simplest way to see this is in terms of the free "momentum shell" states previously defined. For free quarks, these states form complete sets of quark-antiquark states which are good representations of the Lorentz group, so current matrix elements between such shells will have exactly the same Lorentz-covariant structure as the matrix elements of interest (between states of corresponding angular momentum and parity). Now imagine that some matrix element (or linear combination of matrix elements) is of order $(v/c)^n$, n being some nonnegative integer. (In the cases at hand, the one-to-one correspondence between partial-wave amplitudes and Lorentz-invariant amplitudes guarantees the existence of such linear combinations; in the frame $\mathbf{p}_X=0$ introduced earlier, v/c would just be p_B/m_B.) Then integrating such a matrix element over an initial and a final momentum-space wave function (i.e., over ranges of initial and final momentum shells) cannot change this leading behavior: since superpositions such as Eq. (11) are good up to order v/c, the errors in such a calculation will be of *relative* order $(v/c)^2$ and β^2/m^2. [The former error comes from the use of Eq. (11) instead of Eq. (A5), and the latter from the deviations from the strict weak-binding limit.] Thus at zero recoil and in the weak-binding limit, such a calculation will give Lorentz-invariant results.

Surprisingly, one can get Lorentz-invariant results in this kind of situation without even being this careful. Imagine calculating a matrix element such as $\langle\bar{B}(\mathbf{p}_B)|A^m(0)|V(\mathbf{0},s_X)\rangle$ introduced earlier for $m=1,2,3$. Then either $m=1$ or 2 will give [see Eq. (B10)] an equation for the form factor f, whilst $m=3$ will give an equation for the linear combination $f-(a_++a_-)p_B^2$. In Refs. 4 and 5 it was assumed—since f was not calculable by this method to order p_B^2—that these two equations would not determine (a_++a_-). However, we can now see that even such a "brute force" calculation will give the correct answer. The reason is that the matrix element $\langle\bar{B}(\mathbf{p}_B)|A^m(0)|V(\mathbf{0},s_X)\rangle$ can be decomposed into an S-wave part (corresponding to f) and a D-wave part [corresponding to (a_++a_-)], for any choice of $\mathbf{p}_B$, m, and s_X, with coefficients that are (essentially) Clebsch-Gordan coefficients. Since the errors made in computing the S-wave piece will always be the same, they will cancel out in the calculation of (a_++a_-), as long as the $m=1$ (or 2) calculation is carried out to the same order (p_B^2) as the $m=3$ calculation. Incidentally, this means that the "best guess" of Ref. 5 was actually correct. [One can explicitly check that, with their approximations, our Eq. (B17) for a_+ reduces to theirs.]

APPENDIX B: FORMULAS FOR THE FUNCTIONS α, β_{++}, AND γ IN $\bar{B}^0 \to X^+ e \bar{\nu}_e$

We give here the formulas for α, β_{++}, and γ required in Eq. (8) for $d^2\Gamma/dx\,dy$ for $X=q\bar{q}$ in the states $1\,^1S_0$, $1\,^3S_1$, $1\,^3P_2$, $1\,^3P_1$, $1\,^3P_0$, $1\,^1P_1$, $2\,^1S_0$, and $2\,^3S_1$ in the spectroscopic notation $n^{2S+1}L_J$. Throughout the following, we will employ the definitions

$$F_n=\left[\frac{\tilde{m}_X}{\tilde{m}_B}\right]^{1/2}\left[\frac{\beta_B\beta_X}{\beta_{BX}^2}\right]^{n/2} \times\exp\left[-\left[\frac{m_d^2}{4\tilde{m}_B\tilde{m}_X}\right]\frac{t_m-t}{\kappa^2\beta_{BX}^2}\right], \tag{B1}$$

where

$$\beta_{BX}^2=\tfrac{1}{2}(\beta_B^2+\beta_X^2)\ , \tag{B2}$$

$\kappa=0.7$ is the relativistic compensation factor discussed in Sec. II,

$$t_m=(m_B-m_X)^2 \tag{B3}$$

is the maximum momentum transfer, and

$$\mu_\pm=\left[\frac{1}{m_q}\pm\frac{1}{m_b}\right]^{-1}. \tag{B4}$$

Also, we denote by V_μ and A_μ the quark currents $\bar{q}\gamma_\mu b$ and $\bar{q}\gamma_\mu\gamma_5 b$, respectively.

Since, as discussed around Eq. (9), the $\mathbf{p}_X^2$ dependence of the form factors is not calculable accurately, in making a correspondence between $\mathbf{p}_X^2$ and (t_m-t) in the following formulas, we have dropped terms of order $(t_m-t)^2/m^4$ which would correspond to higher-order corrections in (v/c).

1. $1\,^2S_0$

The axial-vector matrix element vanishes, and with

$$\langle X(p_X)|V_\mu|\bar{B}(p_B)\rangle\equiv f_+(p_B+p_X)_\mu+f_-(p_B-p_X)_\mu \tag{B5}$$

we obtain

$$\alpha=\gamma=0 \tag{B6}$$

and

$$\beta_{++}=f_+^2\ , \tag{B7}$$

where

$$f_+=F_3\left[1+\frac{m_b}{2\mu_-}-\frac{m_b m_q}{4\mu_+\mu_-}\frac{m_d}{\tilde{m}_X}\frac{\beta_B^2}{\beta_{BX}^2}\right] \tag{B8}$$

and

$$f_-=F_3\left[1-(\tilde{m}_B+\tilde{m}_X)\left[\frac{1}{2m_q}-\frac{1}{4\mu_+}\frac{m_d}{\tilde{m}_X}\frac{\beta_B^2}{\beta_{BX}^2}\right]\right]. \tag{B9}$$

2. $1\,^3S_1$

With

$$\langle X(p_X,\epsilon)|A_\mu|\bar{B}(p_B)\rangle\equiv f\epsilon_\mu^*+a_+(\epsilon^*\cdot p_B)(p_B+p_X)_\mu +a_-(\epsilon^*\cdot p_B)(p_B-p_X)_\mu \tag{B10}$$

and

$$\langle X(p_X,\epsilon)|V_\mu|\bar{B}(p_B)\rangle \equiv ig\epsilon_{\mu\nu\rho\sigma}\epsilon^{*\nu}(p_B+p_X)^\rho(p_B-p_X)^\sigma \tag{B11}$$

we have

$$\alpha=f^2+4m_B^2g^2\mathbf{p}_X^2\ , \tag{B12}$$

$$\beta_{++}=\frac{f^2}{4m_X^2}-m_B^2g^2y+\tfrac{1}{2}\left[\frac{m_B^2}{m_X^2}(1-y)-1\right]fa_+ +\frac{m_B^2\mathbf{p}_X^2}{m_X^2}a_+^2\ , \tag{B13}$$

and

$$\gamma=2gf\ . \tag{B14}$$

Here $\mathbf{p}_X^2=\{[m_B^2(1-y)+m_X^2]^2/4m_B^2\}-m_X^2$ is the square of the recoil three-momentum of the X. The form factors f, g, and a_+ are given by

$$f=2\tilde{m}_B F_3\ , \tag{B15}$$

$$g=\tfrac{1}{2}F_3\left[\frac{1}{m_q}-\frac{1}{2\mu_-}\frac{m_d}{\tilde{m}_X}\frac{\beta_B^2}{\beta_{BX}^2}\right], \tag{B16}$$

and

$$a_+=-\frac{F_3}{2\tilde{m}_X}\left[1+\frac{m_d}{m_b}\left[\frac{\beta_B^2-\beta_X^2}{\beta_B^2+\beta_X^2}\right]-\frac{m_d^2}{4\mu_-\tilde{m}_B}\frac{\beta_X^4}{\beta_{BX}^4}\right]. \tag{B17}$$

3. $1\,^3P_2$

With

$$\langle X(p_X,\epsilon)|V_\mu|\bar{B}(p_B)\rangle \equiv ih\epsilon_{\mu\nu\lambda\rho}\epsilon^{*\nu\alpha}p_{B_\alpha}(p_B+p_X)^\lambda(p_B-p_X)^\rho \tag{B18}$$

and

$$\langle X(p_X,\epsilon)|A_\mu|\bar{B}(p_B)\rangle \equiv k\epsilon_{\mu\nu}^*p_B^\nu+b_+(\epsilon_{\alpha\beta}^*p_B^\alpha p_B^\beta)(p_B+p_X)_\mu +b_-(\epsilon_{\alpha\beta}^*p_B^\alpha p_B^\beta)(p_B-p_X)_\mu\ , \tag{B19}$$

we have

$$\alpha=\frac{m_B^2\mathbf{p}_X^2}{2m_X^2}(k^2+4m_B^2\mathbf{p}_X^2h^2)\ , \tag{B20}$$

$$\beta_{++}=-\frac{1}{2}y\frac{m_B^4\mathbf{p}_X^2}{m_X^2}h^2+\frac{m_B^2}{24m_X^2}\left[y+\frac{4\mathbf{p}_X^2}{m_X^2}\right]k^2 +\frac{2}{3}\left[\frac{m_B^2\mathbf{p}_X^2}{m_X^2}\right]^2b_+^2+\frac{1}{3}\frac{m_B^2\mathbf{p}_X^2}{m_X^2}\left[\frac{m_B^2}{m_X^2}(1-y)-1\right]kb_+\ , \tag{B21}$$

and

$$\gamma=\frac{m_B^2\mathbf{p}_X^2}{m_X^2}kh \ . \tag{B22}$$

The form factors h, k, and b_+ are given by

$$h=F_5\frac{m_d}{2\sqrt{2}\tilde{m}_B\beta_B}\left[\frac{1}{m_q}-\frac{m_d}{2\tilde{m}_X\mu_-}\frac{\beta_B^2}{\beta_{BX}^2}\right], \tag{B23}$$

$$k=\sqrt{2}F_5\frac{m_d}{\beta_B}, \tag{B24}$$

and

$$b_+=-F_5\frac{m_d}{2\sqrt{2}\tilde{m}_X m_b\beta_B}\left[1-\frac{m_d m_b}{2\mu_+\tilde{m}_B}\frac{\beta_X^2}{\beta_{BX}^2}+\frac{m_d m_b\beta_X^2}{4\tilde{m}_B\mu_-\beta_{BX}^2}\left[1-\frac{m_d\beta_X^2}{2\tilde{m}_B\beta_{BX}^2}\right]\right]. \tag{B25}$$

4. $1\,^3P_1$

The relevant matrix elements are

$$\langle X(p_X,\epsilon)|V_\mu|\bar{B}(p_B)\rangle\equiv l\epsilon_\mu^*+c_+(\epsilon^*\cdot p_B)(p_B+p_X)_\mu+c_-(\epsilon^*\cdot p_B)(p_B-p_X)_\mu \tag{B26}$$

and

$$\langle X(p_X,\epsilon)|A_\mu|\bar{B}(p_B)\rangle\equiv iq\epsilon_{\mu\nu\rho\sigma}\epsilon^{*\nu}(p_B+p_X)^\rho(p_B-p_X)^\sigma \ . \tag{B27}$$

It follows that

$$\alpha=l^2+4m_B^2\mathbf{p}_X^2q^2, \tag{B28}$$

$$\beta_{++}=\frac{l^2}{4m_X^2}-m_B^2yq^2+\tfrac{1}{2}\left[\frac{m_B^2}{m_X^2}(1-y)-1\right]lc_+ +\frac{m_B^2\mathbf{p}_X^2}{m_X^2}c_+^2, \tag{B29}$$

and

$$\gamma=2ql, \tag{B30}$$

where

$$q=\tfrac{1}{2}F_5\frac{m_d}{\tilde{m}_X\beta_B}, \tag{B31}$$

$$l=-F_5\tilde{m}_B\beta_B\left[\frac{1}{\mu_-}+\frac{m_d}{2\tilde{m}_B}\frac{t_m-t}{\kappa^2\beta_B^2}\times\left[\frac{1}{m_q}-\frac{1}{2\mu_-}\frac{m_d}{\tilde{m}_X}\frac{\beta_B^2}{\beta_{BX}^2}\right]\right], \tag{B32}$$

and

$$c_+=F_5\frac{m_d m_b}{4\tilde{m}_B\beta_B\mu_-}\left[1-\frac{m_d m_q}{2\tilde{m}_X\mu_-}\frac{\beta_B^2}{\beta_{BX}^2}\right]. \tag{B33}$$

5. $1\,^3P_0$

The vector matrix element vanishes, and with

$$\langle X(p_X)|A_\mu|\bar{B}(p_B)\rangle\equiv u_+(p_B+p_X)_\mu+u_-(p_B-p_X)_\mu \tag{B34}$$

we have

$$\beta_{++}=u_+^2, \tag{B35}$$

$$\alpha=\gamma=0, \tag{B36}$$

where

$$u_+=F_5\frac{m_d m_q m_b}{\sqrt{6}\beta_B\tilde{m}_X\mu_-} \ . \tag{B37}$$

6. $1\,^1P_1$

The matrix elements of the vector and axial-vector currents have the form

$$\langle X(p_X,\epsilon)|V_\mu|\bar{B}(p_B)\rangle\equiv r\epsilon_\mu^*+s_+(\epsilon^*\cdot p_B)(p_B+p_X)_\mu+s_-(\epsilon^*\cdot p_B)(p_B-p_X)_\mu, \tag{B38}$$

$$\langle X(p_X,\epsilon)|A_\mu|\bar{B}(p_B)\rangle\equiv iv\epsilon_{\mu\nu\rho\sigma}\epsilon^{*\nu}(p_B+p_X)^\rho(p_B-p_X)^\sigma \ . \tag{B39}$$

It follows that

$$\alpha=r^2+4m_B^2\mathbf{p}_X^2v^2 \tag{B40}$$

and

$$\beta_{++}=\frac{r^2}{4m_X^2}-m_B^2yv^2+\frac{1}{2}\left[\frac{m_B^2}{m_X^2}(1-y)-1\right]rs_+ +\frac{m_B^2\mathbf{p}_X^2}{m_X^2}s_+^2, \tag{B41}$$

$$\gamma=2rv, \tag{B42}$$

with

$$v=F_5\frac{\tilde{m}_B\beta_B}{4\sqrt{2}m_b m_q\tilde{m}_X}, \tag{B43}$$

$$r=F_5\frac{\tilde{m}_B\beta_B}{\sqrt{2}\mu_+}, \tag{B44}$$

and

$$s_+=F_5\frac{m_d}{\sqrt{2}\beta_B\tilde{m}_B}\left[1+\frac{m_b}{2\mu_-}-\frac{m_b m_q m_d}{4\mu_+\mu_-\tilde{m}_X}\frac{\beta_B^2}{\beta_{BX}^2}\right]. \tag{B45}$$

7. $2\,^1S_0$

Again the axial-vector contribution vanishes and with

$$\langle X(p_X)|V_\mu|\bar{B}(p_B)\rangle \equiv f'_+(p_B+p_X)_\mu + f'_-(p_B-p_X)_\mu \tag{B46}$$

we have that

$$\alpha=\gamma=0\ , \tag{B47}$$

$$\beta_{++}=f'^2_+\ . \tag{B48}$$

The form factor f'_+ is given by

$$f'_+=F_3\left[\frac{3}{8}\right]^{1/2}\frac{m_b}{\mu_+}\left[\frac{\beta_B^2-\beta_X^2}{\beta_B^2+\beta_X^2} + \frac{m_q m_d}{3\mu_-\tilde{m}_X}\frac{\beta_B^2}{\beta_{BX}^2}\left[\frac{7\beta_X^2-3\beta_B^2}{4\beta_{BX}^2}\right] + \frac{1}{6}\frac{m_d^2}{\tilde{m}_X\tilde{m}_B}\frac{\beta_X^2}{\beta_{BX}^2}\frac{t_m-t}{\kappa^2\beta_{BX}^2} \times\left[1-\frac{m_q m_d}{2\mu_-\tilde{m}_X}\frac{\beta_B^2}{\beta_{BX}^2}\right]\right]\ . \tag{B49}$$

8. $2\,^3S_1$

The matrix elements of the axial-vector and vector currents can be written as

$$\langle X(p_X,\epsilon)|A_\mu|\bar{B}(p_B)\rangle \equiv f'\epsilon^*_\mu + a'_+(\epsilon^*\cdot p_B)(p_B+p_X)_\mu + a'_-(\epsilon^*\cdot p_B)(p_B-p_X)_\mu \tag{B50}$$

and

$$\langle X(p_X,\epsilon)|V_\mu|\bar{B}(p_B)\rangle \equiv ig'\epsilon_{\mu\nu\rho\sigma}\epsilon^{*\nu}(p_B+p_X)^\rho(p_B-p_X)^\sigma\ . \tag{B51}$$

Then we find that

$$\alpha=f'^2+4m_B^2\mathbf{p}_X^2 g'^2\ , \tag{B52}$$

$$\beta_{++}=\frac{f'^2}{4m_X^2}-m_B^2 y g'^2+\frac{1}{2}\left[\frac{m_B^2}{m_X^2}(1-y)-1\right]f'a'_+ + \frac{m_B^2\mathbf{p}_X^2}{m_X^2}a'^2_+\ , \tag{B53}$$

and

$$\gamma=2g'f'\ . \tag{B54}$$

The form factors f', g', a'_+ are given by

$$f'=\sqrt{6}F_3\tilde{m}_B\left[\frac{\beta_B^2-\beta_X^2}{\beta_B^2+\beta_X^2}+\frac{m_d^2}{6\tilde{m}_X\tilde{m}_B}\frac{\beta_X^2}{\beta_{BX}^2}\frac{t_m-t}{\kappa^2\beta_{BX}^2}\right]\ , \tag{B55}$$

$$g'=(\tfrac{3}{8})^{1/2}F_3\left[\left[\frac{\beta_B^2-\beta_X^2}{\beta_B^2+\beta_X^2}+\frac{m_d^2}{6\tilde{m}_X\tilde{m}_B}\frac{\beta_X^2}{\beta_{BX}^2}\frac{t_m-t}{\kappa^2\beta_{BX}^2}\right]\times\left[\frac{1}{m_q}-\frac{m_d}{2\mu_-\tilde{m}_X}\frac{\beta_B^2}{\beta_{BX}^2}\right] + \frac{m_d}{3\mu_-\tilde{m}_X}\frac{\beta_B^2\beta_X^2}{\beta_{BX}^4}\right]\ , \tag{B56}$$

and finally

$$a'_+=\frac{F_5}{\sqrt{6}\tilde{m}_X}\left[\frac{3\tilde{m}_B\beta_{BX}^2}{2m_b\beta_B\beta_X}\left[1-\frac{m_d^2 m_b}{4\tilde{m}_B^2\mu_-}\frac{\beta_X^4}{\beta_{BX}^4}\right]-\frac{3m_d}{2m_b}\frac{\beta_X}{\beta_B} + \frac{5m_d\beta_B\beta_X}{2m_b\beta_{BX}^2}(1+\tfrac{1}{10}T)-\frac{3\tilde{m}_B}{2m_b}\frac{\beta_B}{\beta_X}(1+\tfrac{1}{6}T) + \frac{7m_d^2\beta_B}{8\tilde{m}_B\mu_-\beta_X}\frac{\beta_X^4}{\beta_{BX}^4}(1+\tfrac{1}{14}T)\right]\ , \tag{B57}$$

where

$$T\equiv\frac{m_d^2}{\tilde{m}_X\tilde{m}_B}\frac{\beta_X^2}{\beta_B^2}\frac{t_m-t}{\kappa^2\beta_{BX}^2}\ .$$

APPENDIX C: EXTENDING THE BASIS SPACE

Here we address two issues: (i) the accuracy of our approximate solution of the Coulomb plus linear potential problem and (ii) the convergence of the $b\to u$ expansion as a sum over exclusive channels. They are related because both of them require that we extend our basis space.

In the text, we used simple variational solutions of the Coulomb plus linear potential problem within the $1S$, $1P$, $2S$ basis of harmonic-oscillator states. Here we study the influence on our results of this approximation by obtaining (numerically) exact solutions for S waves. The procedure is to compute the Hamiltonian matrix in the $n_{\max}$ dimensional basis of $1S$, $2S$, ..., $n_{\max}S$ harmonic-oscillator states, to diagonalize this matrix, and to vary the parameter β_S analogous to that appearing in Eq. (15) in order to minimize the ground-state energy. (Of course, as $n_{\max}\to\infty$ this variation becomes unnecessary, but it leads to better convergence.) Then we find

$$|B_n\rangle=\sum_m \alpha_m^{B_n}(\beta_S^B)|B_m^{\rm HO}(\beta_S^B)\rangle\ , \tag{C1}$$

$$|\pi_n\rangle=\sum_m \alpha_m^{\pi_n}(\beta_S^\pi)|\pi_m^{\rm HO}(\beta_S^\pi)\rangle\ , \tag{C2}$$

where $|X_n\rangle$ is the approximately exact nS solution of the Coulomb plus linear problem, and $|X_n^{\rm HO}(\beta)\rangle$ is the nS harmonic-oscillator solution with parameter β. We then have

$$\langle\pi_n|j^\mu(0)|B_1\rangle=\sum_{m'm}\alpha_{m'}^{\pi_n}(\beta_S^\pi)^*\alpha_m^{\beta_1}(\beta_S^B) \times\langle\pi_{m'}^{\rm HO}(\beta_S^\pi)|j^\mu|B_m^{\rm HO}(\beta_S^B)\rangle\ . \tag{C3}$$

The harmonic-oscillator current matrix elements can be

TABLE II. Variational solutions of the Coulomb plus linear problem in the $1S$, $1P$, $2S$ basis. In general, ψ^{1S} and ψ^{2S} mix with some mixing angle θ so that the ground-state wave function is $\cos\theta\psi^{1S}+\sin\theta\psi^{2S}$. For the particular masses and potentials in these systems, θ turns out to be always less than 0.01.

Meson flavor	$u\bar{d}$	$u\bar{s}$	$u\bar{c}$	$u\bar{b}$
β_S (GeV)	0.31	0.34	0.39	0.41
θ		negligible		
β_P (GeV)	0.27	0.30	0.34	

TABLE III. Variational solution of the S-wave Coulomb plus linear problem in the $b \to u$ sector for $n_{\max}=5$. The β value given is the one that minimizes the mass of X_n and therefore gives the best approximation to the state X_n; for this reason the states are only approximately orthogonal for our finite-size basis. Recall that $\langle r_{\bar{d}}^2 \rangle^{1/2} = m\langle r^2 \rangle^{1/2}/(m+\bar{m})$, where the r is the $q\bar{q}$ separation and m ($\bar{m}$) is the mass of the quark (antiquark).

	$\alpha_m^{X_n}$					$\langle r_{\bar{d}}^2 \rangle^{1/2}_{n_{\max}=5}$	$\langle r_{\bar{d}}^2 \rangle^{1/2}_{n_{\max}=2}$	β
X_n	$m=1$	$m=2$	$m=3$	$m=4$	$m=5$	(fm)	(fm)	(GeV)
B_1	0.960	−0.237	+0.141	−0.037	+0.029	0.56	0.55	0.52
π_1	0.965	−0.228	+0.112	−0.031	+0.022	0.39	0.39	0.39
π_2	−0.049	0.977	−0.168	+0.119	0.000	0.72	0.59	0.29
π_3	−0.073	−0.014	0.969	−0.184	+0.148	0.99		0.26
π_4	−0.015	−0.092	−0.152	0.984	0.000	1.21		0.23
π_5	−0.007	−0.018	−0.119	−0.153	0.981	1.43		0.22

computed analytically, giving results analogous to those of Appendix B. The results of this exercise are displayed in Tables II and III and in Fig. 7. Table II gives the β values and expansion coefficients for the $1S$, $1P$, $2S$ bases used for our main results. Table III gives our results for $n_{\max}=5$, by which time we already see convergence. Notice that the value of β is not so relevant physically as the mean distance from the center of mass to the light antiquark, $\langle r_{\bar{d}}^2 \rangle^{1/2}$, which we also tabulate (in the π this distance coincides with the usual naive charge radius). Figure 7 shows explicitly the convergence of the total decay rate of the B to pseudoscalar mesons.

These results also allow us to discuss the accuracy of the harmonic-oscillator truncation (Sec. II) for the $B \to \pi(1S)$ and $B \to \pi(2S)$ transitions. They show that $\Gamma[B \to \pi(1S) e \bar{\nu}_e]$ increased from $0.021|V_{bu}|^2 \times 10^{14}\,\mathrm{sec}^{-1}$ to $0.031|V_{bu}|^2 \times 10^{14}\,\mathrm{sec}^{-1}$ on increasing the basis size sufficiently to produce an accurate solution of the Coulomb plus linear problem. This increase could have been anticipated from Fig. 1, since the more accurate solution was bound to have more high-momentum components than its harmonic approximation, and thus fit the elastic form factor better at higher Q^2. Thus we believe that the more accurate solution is also the more physical one and therefore somewhat more reliable. Since it nevertheless depends on making a model-dependent connection between the pion elastic form factor and the $B \to \pi$ factor, we still do not have the right to expect this rate to be accurate to better than about a factor of 2. Since $B \to \pi(2S)$ is the largest single pseudoscalar rate, we show its convergence explicitly in Table IV.

We have not checked explicitly the variation of our other $b \to u$ rates under an increase of basis size. However, since $B \to \rho(nS)$ is less sensitive to the high-p_X behavior of the form factors, it should be more stable than $B \to \pi(nS)$.

TABLE IV. The $B \to \pi(2S)$ state as a function of basis size, with β chosen to minimize the $\pi(1S)$ mass.

Basis size	$\Gamma(B \to \pi(2S) e \bar{\nu}_e)$ (units of $\lvert V_{bu}\rvert^2 \times 10^{-14}\,\mathrm{sec}^{-1}$)
2×2	0.110
3×3	0.093
4×4	0.089
5×5	0.087
6×6	0.083

APPENDIX D: THE EFFECTS OF RESONANCE WIDTHS

As an example of the effects of resonance widths on our results we have studied the kinematically simplest $\bar{B} \to (\pi\pi)_S e \bar{\nu}_e$ channel, where $(\pi\pi)_S$ denotes that the dipion is in an S wave. This is also arguably the most important case as well as the simplest, since the $\pi\pi$ S-wave phase shift shows a very broad rise from threshold which passes through $\pi/2$ at about 1 GeV: it has been argued (see, for example, Ref. 13) that this broad effect should be associated with the $I=0$, $^3P_0$, $q\bar{q}$ meson expected in the 1.0–1.3-GeV region.

For $(\pi\pi)_S$ production through an S-wave resonance, the invariant amplitude depends only on the mass $m_{\pi\pi}$ of the $\pi\pi$ system and not on its angular orientation with respect to the remaining particles. Therefore, it suffices to convert four-body phase space into an integral over three-body phase space by using

$$\frac{d^3p_1}{2E_1}\frac{d^3p_2}{2E_2} = \frac{d^3p_{\pi\pi}}{2E_{\pi\pi}}\frac{d^3p}{E} = \frac{d^3p_{\pi\pi}}{2E_{\pi\pi}}\frac{1}{4}d\Omega_p dm_{\pi\pi}(m_{\pi\pi}^2 - 4m_\pi^2)^{1/2} . \quad \text{(D1)}$$

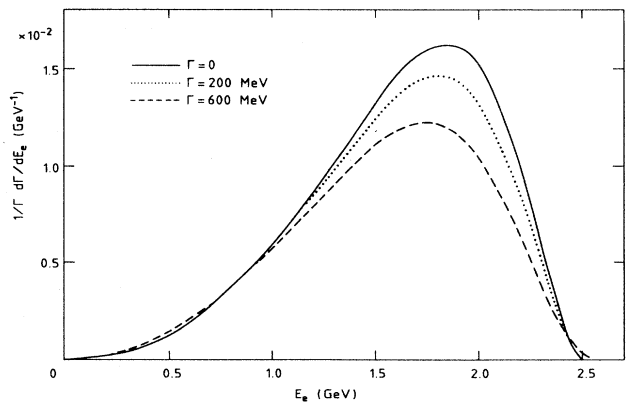

FIG. 8. The effect on the electron spectrum in $\bar{B} \to f_0 e^- \bar{\nu}_e$ of allowing the f_0 to develop a width; $\Gamma=600$ MeV could account for the broad rise of the $\pi\pi$ phase shift from threshold to $\simeq \pi/2$ at 1 GeV.

Here $m_{\pi\pi}=2E$, $\mathbf{p}_{\pi\pi}=\mathbf{p}_1+\mathbf{p}_2$, and $\mathbf{p}=\frac{1}{2}(\mathbf{p}_1^{\rm cm}-\mathbf{p}_2^{\rm cm})$ is in the $\pi\pi$ center-of-mass system. Since the resonance amplitude is independent of Ω_p, the angles associated with $\mathbf{p}$, we just get, for a resonance of mass m_0,

$$\frac{d^2\Gamma(\bar{B}\to(\pi\pi)_S e^-\bar{\nu}_e)}{dx\,dy} = \frac{1}{\pi}\int dm_{\pi\pi}^2 \frac{m_0\Gamma_0(m_{\pi\pi}^2)}{(m_{\pi\pi}^2-m_0^2)^2+m_0^2\Gamma_0^2(m_{\pi\pi}^2)} \times \frac{d^2\Gamma(\bar{B}\to X_0 e^-\bar{\nu}_e)}{dx\,dy}, \quad \text{(D2)}$$

where $m_0\Gamma_0(m_{\pi\pi}^2)=(g^2/16\pi m_{\pi\pi})(m_{\pi\pi}^2-4m_\pi^2)^{1/2}$, and $d^2\Gamma(\bar{B}\to X_0 e\bar{\nu}_e)/dx\,dy$ is the rate for decay to a stable scalar particle of mass $m_{\pi\pi}$.

The effect of Eq. (D2) on the $\bar{B}\to f_0 e\bar{\nu}_e$ electron spectrum is shown in Fig. 8. For $\Gamma_{f_0}(m_{f_0})<200$ MeV/c^2, the change in $d\Gamma/dE_e$ is almost unnoticeable ($\lesssim 5\%$). For a very broad resonance of mass 1.09 GeV/c^2 and width 600 MeV/c^2 (see Table I) there is about a 20% depletion in the total rate (the Breit-Wigner tail at low mass gets "lost" below threshold). Most relevant for us, however, is the fact that there is no significant additional contribution to the high-energy electron spectrum from the low $m_{\pi\pi}$ tail of such a broad resonance.

*Present address: Fermilab, Theory Group, P.O. Box 500, Batavia, Illinois 60565.

[1]See the review by E. H. Thorndike, in *Proceedings of the 1985 International Symposium at High Energies,* Kyoto, Japan, 1985, edited by M. Konuma and K. Takahashi (Research Institute for Fundamental Physics, Kyoto University, 1986), p. 406.

[2]G. Altarelli, M. Cabibbo, G. Corbo, and L. Maiani, Nucl. Phys. **B207**, 365 (1982); N. Cabibbo, G. Corbo, and L. Maiani, *ibid.* **B155**, 93 (1979). See also Refs. 15.

[3]B. Grinstein, M. B. Wise, and N. Isgur, Phys. Rev. Lett. **56**, 258 (1986).

[4]B. Grinstein, M. B. Wise, and N. Isgur, Caltech Report No. CALT-68-1311, and University of Toronto Report No. UTPT-85-37, 1985 (unpublished).

[5]T. Altomari and L. Wolfenstein, Phys. Rev. Lett. **58**, 1583 (1987).

[6]M. Kobayashi and T. Maskawa, Prog. Theor. Phys. **49**, 652 (1973).

[7]A. Donnachie, G. Shaw, and D. Lyth, in *Electromagnetic Interactions of Hadrons,* edited by A. Donnachie and G. Shaw (Plenum, New York, 1978); G. von Gehlen, H. Wessel, and H. Rubinstein, Phys. Lett. **42B**, 365 (1972); E. Bloom and F. Gilman, Phys. Rev. Lett. **25**, 1140 (1970).

[8]R. Kokoski and N. Isgur, Phys. Rev. D **35**, 907 (1987), and references therein.

[9]N. Isgur (work in progress).

[10]N. Isgur, Phys. Rev. D **12**, 3666 (1975); C. Hayne and N. Isgur, *ibid.* **25**, 1944 (1982); N. Isgur, Acta Phys. Pol. **B6**, 1081 (1977).

[11]M. B. Voloshin and M. A. Shifman, Yad. Fiz. **45**, 463 (1987) [Sov. J. Nucl. Phys. **45**, 292 (1987)]; H. D. Politzer and M. B. Wise, Phys. Lett. B **206**, 681 (1988). G. P. Lepage and B. A. Thacker, Cornell Report No. CLNS 87/114, 1987; in *Field Theory on the Lattice,* proceedings of the International Symposium, Seillac, France, 1987, edited by A. Billoire *et al.* [Nucl. Phys. B, Proc. Suppl. **4** (1988)].

[12]Particle Data Group, M. Aguilar-Benitez *et al.*, Phys. Lett. **B170**, 1 (1986).

[13]S. Godfrey and N. Isgur, Phys. Rev. D **32**, 189 (1985). Reference 8 contains a more fundamental and more complete discussion of decays.

[14]C. J. Bebek *et al.*, Phys. Rev. D **17**, 1693 (1978).

[15]M. K. Gaillard, B. W. Lee, and J. L. Rosner, Rev. Mod. Phys. **47**, 277 (1975); J. Ellis, M. K. Gaillard, and D. V. Nanopoulos, Nucl. Phys. **B100**, 313 (1975).

[16]I. Hinchliffe and C. H. Llewellyn Smith, Nucl. Phys. **B114**, 45 (1976); V. Barger, T. Gottschalk, and R. J. N. Phillips, Phys. Rev. D **16**, 746 (1977); G. K. Lane, Phys. Lett. **70B**, 227 (1977); M. B. Gavela, *ibid.* **83B**, 367 (1979); F. E. Close, G. J. Gounaris, and J. Paschalis, *ibid.* **149B**, 209 (1984); M. Suzuki, *ibid.* **155B**, 112 (1985); S. Nussinov and W. Wetzel, Phys. Rev. D **36**, 130 (1987); see also Ref. 5.

[17]W. Wirbel, B. Stech, and M. Bauer, Z. Phys. C **29**, 637 (1985); J. G. Körner and G. A. Shuler, *ibid.* **38**, 511 (1988).

[18]A. Ali and T. C. Yang, Phys. Lett. **65B**, 275 (1976); D. Fakirov and B. Stech, Nucl. Phys. **B133**, 315 (1978); S. C. Chao, G. Kramer, W. F. Palmer, and S. S. Pinsky, Phys. Rev. D **30**, 1916 (1984).

[19]F. Bletzacker, M. T. Nieh, and A. Soni, Phys. Rev. D **16**, 732 (1977); Y. Kizikuri, Prog. Theor. Phys. **67**, 1598 (1982).

[20]M. Ademollo and R. Gatto, Phys. Rev. Lett. **13**, 264 (1964).

[21]W. Bacino *et al.*, Phys. Rev. Lett. **43**, 1073 (1979).

[22]Mark III Collaboration, D. M. Coffman, in *Hadron Spectroscopy—1985,* proceedings of the International Conference, College Park, Maryland, edited by S. Oneda (AIP Conf. Proc. No. 132) (AIP, New York, 1985), p. 322; Caltech Ph.D. thesis, 1986; Report No. CALT-68-1415, 1987 (unpublished); Mark III Collaboration, R. H. Schindler, in *Proceedings of the 23rd International Conference on High-Energy Physics,* Berkeley, 1986, edited by S. C. Loken (World Scientific, Singapore, 1987), p. 745.

[23]D. Hitlin, in *Proceedings of the International Symposium on Production and Decay of Heavy Hadrons,* Heidelberg, 1986, edited by K. R. Schubert and R. Waldi (DESY, Hamburg, 1986), p. 105.

[24]B. Grinstein and M. B. Wise, Phys. Lett. B **197**, 249 (1987).

[25]Note that the inclusion of a_+ has improved the fit to the electron spectrum relative to that given in Ref. 4.

[26]T. Altomari and L. Wolfenstein, Phys. Rev. D **37**, 681 (1988).

[27]CLEO Collaboration, S. E. Csorna *et al.*, in *Lepton and Photon Interactions,* proceedings of the International Symposium on Lepton and Photon Interactions at High Energies, Hamburg, W. Germany, 1987, edited by W. Bartel and R. Rückl [Nucl. Phys. B Proc. Suppl. **3** (1988)].

[28]CUSB Collaboration, C. Klopfenstein *et al.*, Phys. Lett. **130B**, 444 (1983).

[29]CLEO Collaboration, A. Chen *et al.*, Phys. Rev. Lett. **52**, 1084 (1984).

[30]ARGUS Collaboration, S. Weseler, in *Proceedings of the International Symposium on Production and Decay of Heavy Hadrons* (Ref. 23), p. 119.

[31]CLEO Collaboration, S. Behrends *et al.*, Phys. Rev. Lett. **59**, 407 (1987).

[32]ARGUS Collaboration, K. R. Schubert, in *Proceedings of the 23rd International Conference on High-Energy Physics* (Ref. 22), p. 781.

[33]Crystal Ball Collaboration, K. Wachs, in *Hadron, Quarks and Gluons,* proceedings of the 22nd Rencontres de Moriond, Les Arcs, France, 1987 edited by J. Tran Thanh Van (Editions Frontières, Gif-sur-Yvette, 1987); Crystal Ball Collaboration, T. Skwanicki, in *Proceedings of the 23rd International Conference on High Energy Physics* (Ref. 22), p. 778.